R. & M. No. 3195

R. & M. No. 3195
(20,373)
A.R.C. Technical Report

MINISTRY OF AVIATION

AERONAUTICAL RESEARCH COUNCIL
REPORTS AND MEMORANDA

Combined Flexure and Torsion of a Class of Heated Thin Wings: A Large-Deflection Analysis

By E. H. MANSFIELD, Sc.D.

LONDON: HER MAJESTY'S STATIONERY OFFICE
1961
PRICE 11s. 6d. NET

Combined Flexure and Torsion of a Class of Heated Thin Wings: A Large-Deflection Analysis

By E. H. Mansfield, Sc.D.

Communicated by the Director-General of Scientific Research (Air)
Ministry of Supply

*Reports and Memoranda No. 3195**
March, 1958

Summary.—This paper presents a large-deflection analysis for combined flexure and torsion of solid or hollow wings of biconvex section with a parabolic chordwise temperature distribution. The analysis embraces the buckled, as well as unbuckled, regimes.

1. *Introduction.*—One of the problems arising from the aerodynamic heating of a wing is that thermal stresses may reduce the overall stiffness of the wing. Aerodynamic heating of a solid wing produces chordwise variations of temperature which give rise to a thermal stress distribution which is characterised by spanwise compressive stresses at the leading and trailing edges and equilibrating tensile stresses at the mid-chord. If the wing remains perfectly flat these middle-surface stresses are completely self-equilibrating; but if the wing is twisted the middle-surface stresses have a resultant torque acting in the same sense as the twist and this results in an effective reduction of the torsional rigidity.[1, 2, 3, 4, 5, 6] If the wing is bent its cross-section distorts because of the anticlastic effect and because of the radial component of the middle-surface stresses. Because of this distortion the middle-surface stresses now have a resultant moment acting in the same sense as the applied moment and this results in an effective reduction of the flexural rigidity.[6, 7]

The present paper gives the large-deflection analysis for combined flexure and torsion of a class of heated thin wings of infinite aspect ratio. The non-linear character of this large-deflection analysis stems from the fact that the middle-surface forces can result from, or be modified by, changes in the spanwise curvature or in the twist per unit length.

Because of the comparative simplicity of the present analysis it has been possible to extend the investigation of the wing behaviour outside the normal practical range. Thus the investigation includes a consideration of the following phenomena: 'positive' and 'negative' (e.g., 'heating' and 'cooling') thermal buckling and post-buckling behaviour, torsional buckling and post-buckling behaviour modified by thermal effects, and flexural snap-through buckling of a 'negatively' thermally buckled wing.

* R.A.E. Report Structures 237, received 2nd September, 1958.

2. *Method of Analysis.*—In order to determine the relationships between bending moment, torque, spanwise curvature and twist it is first necessary to determine the chordwise distortion of the wing subject to a given (arbitrary) spanwise curvature and twist. The differential equation which governs this distortion is determined in Section 2.1. The solution of this differential equation for wings of parabolic lenticular section with a parabolic chordwise variation of temperature is given in Section 2.2. The strain energy per unit length of wing is then determined in Section 2.3 in terms of the spanwise curvature and twist; the bending moment and torque may thus be readily found by differentiation of the strain energy with respect to the curvature and twist.

2.1. *Derivation of the Differential Equation.*—The chordwise variation of the distortion of the wing may be determined most conveniently by variational methods. Consider first a wing with arbitrary chordwise thickness variation and arbitrary solidity subjected to a spanwise curvature κ and twist per unit length θ. The distortion of the wing is then of the form

$$w(x, y) = \tfrac{1}{2}\kappa y^2 + \theta xy + w(x), \tag{1}$$

where the chordwise distortion of the wing $w(x)$, hereafter referred to simply as w, may be determined from energy considerations.

The strain energy due to spanwise strains in the middle surface of the wing will now be determined. The first term on the right-hand side of equation (1) represents a developable surface and therefore contributes no middle-surface strains. The second term in equation (1) gives rise to spanwise strains that vary as $\frac{1}{2}\theta^2 x^2$. The final term in equation (1) gives rise to strains that vary as $-\kappa w$. The spanwise strain (measured from a stress-free datum) is thus given by

$$\epsilon = \bar{\epsilon} + \tfrac{1}{2}\theta^2 x^2 - \kappa w + A_1 + A_2 x, \tag{2}$$

where the constants A_1 and A_2 are such that there is spanwise equilibrium, i.e.,

$$\left.\begin{aligned} \int_{-a/2}^{a/2} E\epsilon\bar{t}\, dx &= 0 \\ \int_{-a/2}^{a/2} xE\epsilon\bar{t}\, dx &= 0 \end{aligned}\right\}. \tag{3}$$

For simplicity equation (2) is written in the form

$$\epsilon = \bar{\epsilon}' - \kappa w, \tag{4}$$

where $\bar{\epsilon}'$ is independent of w. There are no chordwise middle-surface stresses so the strain energy per unit length due to the middle-surface strains is given by

$$V_m = \tfrac{1}{2}\int_{-a/2}^{a/2} E\bar{t}(\bar{\epsilon}' - \kappa w)^2\, dx. \tag{5}$$

The strain energy per unit length due to flexure and torsion[8] is given by

$$\begin{aligned} V_f &= \tfrac{1}{2}\int_{-a/2}^{a/2} D\left[\{\nabla^2 w(x, y)\}^2 - 2(1-\nu)\left\{\frac{\partial^2 w(x, y)}{\partial x^2}\,\frac{\partial^2 w(x, y)}{\partial y^2} - \left(\frac{\partial^2 w(x, y)}{\partial x\,\partial y}\right)^2\right\}\right] dx \\ &= \tfrac{1}{2}\int_{-a/2}^{a/2} D\left\{\left(\frac{\partial^2 w}{\partial x^2}\right)^2 + 2\nu\kappa\frac{\partial^2 w}{\partial x^2} + \kappa^2 + 2(1-\nu)\theta^2\right\} dx \end{aligned} \tag{6}$$

by virtue of equation (1).

The total strain energy per unit length is the sum of these two and the condition that this is a minimum with respect to w requires[9] w to satisfy the following differential equation

$$\frac{d^2}{dx^2}\left\{D\left(\frac{d^2w}{dx^2}+\nu\kappa\right)\right\}-E\kappa\bar{t}(\bar{\epsilon}'-\kappa w)=0. \tag{7}$$

The four boundary conditions appropriate to this equation express the fact that the leading and trailing edges are free, whence

$$\left.\begin{aligned}\left[D\left(\frac{d^2w}{dx^2}+\nu\kappa\right)\right]_{x=\pm a/2}&=0\\ \left[\frac{d}{dx}\left\{D\left(\frac{d^2w}{dx^2}+\nu\kappa\right)\right\}\right]_{x=\pm a/2}&=0\end{aligned}\right\}. \tag{8}$$

2.2. *Wings of Parabolic Lenticular Section and Parabolic Temperature Variation.*—In this paragraph the solution of equation (7) will be derived for wings of solid section and for wings of thin walled section with a stabilising filling (so that the wing acts as a 'plate' instead of a hollow tube). Throughout it is assumed that Young's modulus E and the coefficient of thermal expansion α do not vary with temperature.

2.2.1. *Solid wings.*—For such wings

$$\left.\begin{aligned}\bar{t}&=t_0\left\{1-\left(\frac{2x}{a}\right)^2\right\}\\ D&=D_0\left\{1-\left(\frac{2x}{a}\right)^2\right\}^3\\ D_0&=\frac{Et_0^{\,3}}{12(1-\nu^2)}\end{aligned}\right\}, \tag{9}$$

and if

$$T=T_0+T_1\left(\frac{2x}{a}\right)+\Delta T\left(\frac{2x}{a}\right)^2, \tag{10}$$

it follows from equations (2), (3) and (9) that

$$\bar{\epsilon}=\alpha\Delta T\left\{\frac{1}{5}-\left(\frac{2x}{a}\right)^2\right\}. \tag{11}$$

In a similar manner it can be shown that

$$\bar{\epsilon}'=\left(\alpha\Delta T-\frac{a^2\theta^2}{8}\right)\left\{\frac{1}{5}-\left(\frac{2x}{a}\right)^2\right\}, \tag{12}$$

so that equation (7) becomes

$$D_0\frac{d^2}{dx^2}\left[\left\{1-\left(\frac{2x}{a}\right)^2\right\}^3\left(\frac{d^2w}{dx^2}+\nu\kappa\right)\right]-$$
$$-E\kappa t_0\left\{1-\left(\frac{2x}{a}\right)^2\right\}\left[\left(\alpha\Delta T-\frac{a^2\theta^2}{8}\right)\left\{\frac{1}{5}-\left(\frac{2x}{a}\right)^2\right\}-\kappa w\right]=0. \tag{13}$$

It can be readily verified that the solution of equation (13) which satisfies the boundary conditions (8) is

$$w = \frac{\frac{\kappa a^2}{8}\left(\nu+\frac{Ea^2t_0(8\alpha\Delta T-a^2\theta^2)}{960D_0}\right)\left\{\frac{1}{5}-\left(\frac{2x}{a}\right)^2\right\}}{1+\frac{Ea^4\kappa^2t_0}{960D_0}} \tag{14}$$

and it will be noticed that the chordwise curvature $\kappa'(=d^2w/dx^2)$ is constant.

2.2.2. *Thin-walled wing.*—The wing is assumed to have an outer skin covering of constant thickness h and a stabilising and shear resistant filling (such as a honeycomb). The contribution of this filling in resisting straining of the middle surface and overall bending is ignored.

For such wings

$$\left.\begin{aligned} \bar{t} &= 2h \\ D &= D_0\left\{1-\left(\frac{2x}{a}\right)^2\right\}^2 \\ D_0 &= \frac{Eht_0^2}{2(1-\nu^2)} \end{aligned}\right\} \tag{15}$$

while, from equations (2), (3) and (15),

$$\bar{\epsilon}' = \left(\alpha\Delta T-\frac{a^2\theta^2}{8}\right)\left\{\frac{1}{3}-\left(\frac{2x}{a}\right)^2\right\}. \tag{16}$$

Equation (7) therefore becomes

$$D_0\frac{d^2}{dx^2}\left[\left\{1-\left(\frac{2x}{a}\right)^2\right\}^2\left(\frac{d^2w}{dx^2}+\nu\kappa\right)\right]-2E\kappa h\left[\left(\alpha\Delta T-\frac{a^2\theta^2}{8}\right)\left\{\frac{1}{3}-\left(\frac{2x}{a}\right)^2\right\}\right]-\kappa w = 0. \tag{17}$$

It can be readily verified that the solution of equation (17) which satisfies the boundary conditions (8) is

$$w = \frac{\frac{\kappa a^2}{8}\left(\nu+\frac{Ea^2h(8\alpha\Delta T-a^2\theta^2)}{192D_0}\right)\left\{\frac{1}{3}-\left(\frac{2x}{a}\right)^2\right\}}{1+\frac{Ea^4\kappa^2h}{192D_0}} \tag{18}$$

and it will be noticed that the chordwise curvature κ' is constant.

2.3. *Strain Energy in the Wing.*—The strain energy per unit length of wing may now be obtained by substituting equation (14) or (18) in equations (5) and (6). The strain energy per unit length so obtained is a function of the wing structure, the temperature difference ΔT, and the curvatures κ and θ. The bending moment M and the torque T may therefore be obtained by differentiating:

$$M = \frac{\partial V}{\partial \kappa}$$

and

$$T = \frac{\partial V}{\partial \theta},$$

where

$$V = V_m+V_f \tag{19}$$

At this stage, however, it is convenient to introduce the following non-dimensional parameters:

(a) *Solid wing*

$$\left.\begin{aligned}
\hat{V} &= \left(\frac{21a^3}{64Et_0^5}\right) V \\
\hat{\sigma} &= \frac{a^2\alpha\Delta T}{10t_0^2} \\
\hat{\kappa} &= \left(\frac{a^2}{(4\sqrt{5})\,t_0}\right) \kappa \\
\hat{\theta} &= \left(\frac{a^2}{(4\sqrt{5})\,t_0}\right) \theta \\
\hat{M} &= \left(\frac{(21\sqrt{5})\,a}{16Et_0^4}\right) M \\
\hat{T} &= \left(\frac{(21\sqrt{5})\,a}{64Gt_0^4}\right) T \\
\hat{\kappa}' &= \left(\frac{a^2}{(4\sqrt{5})\,t_0}\right) \kappa'
\end{aligned}\right\}. \tag{20}$$

(b) *Thin-walled wing*

$$\left.\begin{aligned}
\hat{V} &= \left(\frac{5a^3}{128Eht_0^4}\right) V \\
\hat{\sigma} &= \frac{a^2\alpha\Delta T}{12t_0^2} \\
\hat{\kappa} &= \left(\frac{a^2}{(4\sqrt{6})\,t_0}\right) \kappa \\
\hat{\theta} &= \left(\frac{a^2}{(4\sqrt{6})\,t_0}\right) \theta \\
\hat{M} &= \left(\frac{(5\sqrt{6})\,a}{32Eht_0^3}\right) M \\
\hat{T} &= \left(\frac{(5\sqrt{6})\,a}{128Ght_0^3}\right) T \\
\hat{\kappa}' &= \left(\frac{a^2}{(4\sqrt{6})\,t_0}\right) \kappa'
\end{aligned}\right\}. \tag{21}$$

Hereafter, only non-dimensional symbols, all of which have circumflexes, are employed and all the remaining equations are applicable to both solid and thin-walled wings.

2.3.1. *Solid and thin-walled wings.*—The strain energy per unit length is now given by

$$\hat{V} = \tfrac{1}{2}\hat{\kappa}^2 + \frac{\hat{\theta}^2}{1+\nu} + \frac{(\hat{\sigma}-\hat{\theta}^2-\nu\hat{\kappa}^2)^2}{2\{1+(1-\nu^2)\,\hat{\kappa}^2\}} \tag{22}$$

and the chordwise curvature by

$$\hat{\kappa}' = -\left(\frac{\nu+(1-\nu^2)\,(\hat{\sigma}-\hat{\theta}^2)}{1+(1-\nu^2)\,\hat{\kappa}^2}\right)\hat{\kappa}. \tag{23}$$

All the remaining equations are deduced from these two relations. The bending moment and torque, from equations (19), (20) or (21), are given by

$$\left.\begin{aligned}\hat{M} &= \frac{\partial \hat{V}}{\partial \hat{\kappa}} \\ \hat{T} &= \left(\frac{1+\nu}{2}\right)\frac{\partial \hat{V}}{\partial \hat{\theta}}\end{aligned}\right\} \tag{24}$$

and it will be noted that on small deflection theory, with $\hat{\sigma}$ zero

$$\hat{M} = \hat{\kappa}$$

$$\hat{T} = \hat{\theta}.$$

3. *General Relations Between $\hat{\kappa}$, $\hat{\theta}$, $\hat{M}$, $\hat{T}$.*—The bending moment and torque may be expressed in terms of the longitudinal curvature and the twist per unit length by virtue of equations (22) and (24). Thus,

$$\hat{M} = \frac{\hat{\kappa}\{1-(1+\nu)(\hat{\sigma}-\hat{\kappa}^2-\hat{\theta}^2)\}\{1+(1-\nu)(\hat{\sigma}+\hat{\kappa}^2-\hat{\theta}^2)\}}{\{1+(1-\nu^2)\hat{\kappa}^2\}^2} \tag{25}$$

$$\hat{T} = \frac{\hat{\theta}\{1-(1+\nu)(\hat{\sigma}-\hat{\kappa}^2-\hat{\theta}^2)\}}{\{1+(1-\nu^2)\hat{\kappa}^2\}} \tag{26}$$

Further, by virtue of these relations, it can be shown that

$$\frac{\hat{M}}{\hat{\kappa}} = \frac{\hat{T}}{\hat{\theta}}\left\{\frac{2}{1+\nu} - \left(\frac{1-\nu}{1+\nu}\right)\frac{\hat{T}}{\hat{\theta}}\right\} \tag{27}$$

which is independent of $\hat{\sigma}$.

It is clear from these relations and from the physical aspects of the problem, that for given values of $\hat{\kappa}$ and $\hat{\theta}$ there exist unique values for $\hat{M}$ and $\hat{T}$, but the converse is not necessarily true (i.e., given values of $\hat{M}$ and $\hat{T}$ may be possible with more than one pair of values for $\hat{\kappa}$ and $\hat{\theta}$). This is demonstrated in Figs. 2 to 17 where curves of constant $\hat{\kappa}$ and constant $\hat{\theta}$ have been plotted against $\hat{M}$ and $\hat{T}$ for various values of $\hat{\sigma}$.

Fig. 18 shows the regions in the $\hat{M}$, $\hat{T}$ plane in which $\hat{\kappa}$ and $\hat{\theta}$ do not have unique values. For values of $\hat{\sigma}$ less than $-1/(1-\nu)$ there is one region in which $\hat{\kappa}$ and $\hat{\theta}$ do not have unique values and two regions in which $\hat{\kappa}$ and $\hat{\theta}$ have unique values. For values of $\hat{\sigma}$ greater than $-1/(1-\nu)$ but less than $1/(1+\nu)$ there are two regions in which $\hat{\kappa}$ and $\hat{\theta}$ do not have unique values and one region in which $\hat{\kappa}$ and $\hat{\theta}$ have unique values. For values of $\hat{\sigma}$ greater than $1/(1+\nu)$ there are three regions in which $\hat{\kappa}$ and $\hat{\theta}$ do not have unique values and one region in which $\hat{\kappa}$ and $\hat{\theta}$ have unique values. In all cases increasing the value of $|\hat{M}|$ has a stabilising effect.

4. *Special Cases.*—4.1. *Condition of Zero Moment and Zero Torque.*—The problem here is to determine the distortion of an unloaded wing due to thermal buckling. The condition of zero $\hat{M}$ and zero $\hat{T}$ is obtained from equations (25) and (26) and determines certain relationships between $\hat{\kappa}$ and $\hat{\theta}$:

$$\left.\begin{aligned}\hat{\kappa}\{1-(1+\nu)(\hat{\sigma}-\hat{\kappa}^2-\hat{\theta}^2)\}\{1+(1-\nu)(\hat{\sigma}+\hat{\kappa}^2-\hat{\theta}^2)\} &= 0 \\ \hat{\theta}\{1-(1+\nu)(\hat{\sigma}-\hat{\kappa}^2-\hat{\theta}^2)\} &= 0\end{aligned}\right\}. \tag{28}$$

There are thus three possible states, namely:

(i)
$$\left.\begin{array}{l}\hat{\kappa} = 0 \\ \hat{\theta} = 0\end{array}\right\}, \tag{29}$$

or (ii)
$$1-(1+\nu)(\hat{\sigma}-\hat{\kappa}^2-\hat{\theta}^2) = 0, \tag{30}$$

or (iii)
$$\left.\begin{array}{r}1+(1-\nu)(\hat{\sigma}+\hat{\kappa}^2) = 0 \\ \hat{\theta} = 0\end{array}\right\}, \tag{31}$$

A comparison of strain energies shows which of these three states is the correct one. First, however, it must be noticed that, because $\hat{\kappa}^2$ and $\hat{\theta}^2$ are essentially positive, state (ii) is possible only if

$$\hat{\sigma} > \frac{1}{1+\nu} \tag{32}$$

and state (iii) is possible only if

$$\hat{\sigma} < \frac{-1}{1-\nu}. \tag{33}$$

The strain energies corresponding to these three possible states are found from equation (22) and are given by

$$\left.\begin{array}{l}\hat{V}_{(i)} = \frac{1}{2}\hat{\sigma}^2 \\ \hat{V}_{(ii)} = \frac{1}{2}\hat{\sigma}^2-\dfrac{1}{2}\left(\hat{\sigma}-\dfrac{1}{1+\nu}\right)^2 \\ \hat{V}_{(iii)} = \frac{1}{2}\hat{\sigma}^2-\dfrac{1}{2}\left(\hat{\sigma}+\dfrac{1}{1-\nu}\right)^2\end{array}\right\} \tag{34}$$

and it follows from equations (32), (33) and (34) that state (ii) exists when condition (32) holds, state (iii) exists when condition (33) holds, otherwise state (i) exists and the wing does not buckle.

It is to be noticed that equation (30) permits an infinite variety of distorted shapes, but this is a special case (in an actual wing the end effects will tend to put a premium on the purely twisted shape). Generally, if there is more than one possible configuration, it will be found that there are two stable states and one unstable state. For example, if $\hat{\sigma} < -1/(1-\nu)$ the two stable states correspond to the positive and negative roots of equation (31), and the unstable state corresponds to condition (29).

The chordwise curvature corresponding to the buckled states (ii) and (iii) is given by equations (23), (30) and (31). In terms of the spanwise curvature $\hat{\kappa}$, it is found that

$$\hat{\kappa}'_{(ii)} = -\hat{\kappa}, \tag{35}$$

$$\hat{\kappa}'_{(iii)} = +\hat{\kappa}. \tag{36}$$

4.2. *Pure Moment*.—The condition that $\hat{T}$ is zero and $\hat{M}$ non-zero implies that $\hat{\theta}$ is zero. Equation (25) then yields

$$\left.\begin{array}{l}\hat{M} = \dfrac{\hat{\kappa}\{1-(1+\nu)(\hat{\sigma}-\hat{\kappa}^2)\}\{1+(1-\nu)(\hat{\sigma}+\hat{\kappa}^2)\}}{\{1+(1-\nu^2)\hat{\kappa}^2\}^2} \\ \quad \equiv \dfrac{\hat{\kappa}}{(1-\nu^2)}\left\{1-\left(\dfrac{\nu+(1-\nu^2)\hat{\sigma}}{1+(1-\nu^2)\hat{\kappa}^2}\right)^2\right\}\end{array}\right\}. \tag{37}$$

This bending moment-curvature relationship has been plotted in Fig. 19 for various values of $\hat{\sigma}$. A number of special cases warrant attention. If there are no thermal stresses

$$\hat{M} = \frac{\hat{\kappa}}{(1-\nu^2)}\left\{1-\left(\frac{\nu}{1+(1-\nu^2)\hat{\kappa}^2}\right)^2\right\}, \tag{38}$$

which is the ordinary large-deflection solution.

If

$$\hat{\sigma} = \frac{-\nu}{1-\nu^2},$$

it follows that

$$\hat{M} = \frac{\hat{\kappa}}{1-\nu^2}, \tag{39}$$

which corresponds to the solution on 'inextensional' plate theory.[10] The reason for this is that the radial component of the middle-surface stresses exactly counteracts the anti-clastic effect, so that $\hat{\kappa}'$ is zero. In general, as $\hat{\kappa}$ increases the bending moment-curvature relationship tends towards equation (39), for all values of $\hat{\sigma}$.

4.2.1. *Snap-through flexural buckling.*—If the wing was originally in state (iii) so that

$$\left.\begin{aligned} &\hat{\sigma} < \frac{-1}{1-\nu} \\ \text{and} \quad &\hat{\kappa}_0 = \pm\left(-\hat{\sigma}-\frac{1}{1-\nu}\right)^{1/2} \end{aligned}\right\}, \tag{40}$$

a violent flexural instability will occur at a critical value of $\hat{M}$ if $\hat{M}$ and $\hat{\kappa}_0$ are of opposite sign (the mechanism of this instability is similar to that in a toy metal 'clicker'). For purposes of argument $\hat{\kappa}_0$ will be assumed negative and $\hat{M}$ positive. As $\hat{M}$ increases $\hat{\kappa}$ increases so that, because of the negative sign of $\hat{\kappa}_0$, $|\hat{\kappa}|$ decreases. But $\hat{M}$ is zero when $\hat{\kappa}$ is zero and therefore there is a critical negative value $\hat{\kappa}^*$ at which the positive moment $\hat{M}^*$ is a maximum. A further increase in the value of $\hat{M}$ causes the wing to snap through to a positive value of $\hat{\kappa}$. It can be shown by differentiating equation (37) that

$$\left.\begin{aligned} &(1-\nu^2)(\hat{\kappa}^*)^2 = \mu^{1/3}[\{\sqrt{(4+\mu)}+2\}^{1/3}-\{\sqrt{(4+\mu)}-2\}^{1/3}]-1 \\ \text{where} \quad &\mu = \{\nu+(1-\nu^2)\hat{\sigma}\}^2 \end{aligned}\right\} \tag{41}$$

and hence $\hat{M}^*$ can be determined.

4.2.2. *Flexural rigidity.*—A non-dimensional measure of the flexural rigidity is afforded by the symbol $\hat{S}_M$ where

$$\hat{S}_M = \left(\frac{\partial \hat{M}}{\partial \hat{\kappa}}\right)_{\hat{T}=\text{const}} \tag{42}$$

and for the special case of pure moment considered in this paragraph it is obtained by differentiating equation (37). The initial value of the flexural rigidity (i.e., at $\hat{M} = 0$) is determined from this relation using the results of Section 4.1. The stiffness depends markedly on whether the wing is in state (i), (ii) or (iii). In the unbuckled state (i) for which

$$\left.\begin{aligned} &\frac{-1}{1-\nu} < \hat{\sigma} < \frac{1}{1+\nu} \\ \text{it can be shown that} \quad &\hat{S}_{M,0} = \{1-(1+\nu)\hat{\sigma}\}\{1+(1-\nu)\hat{\sigma}\} \end{aligned}\right\}. \tag{43}$$

In the buckled state (ii) for which

it can be shown that

$$\left.\begin{aligned} \hat{\sigma} &> \frac{1}{1+\nu} \\ \hat{S}_{M,0} &= \frac{4\left(\hat{\sigma}-\dfrac{1}{(1+\nu)}\right)}{\nu+(1-\nu^2)\hat{\sigma}} \\ &\text{or} \quad 0 \end{aligned}\right\}, \tag{44}$$

and in the buckled state (iii) for which

it can be shown that

$$\left.\begin{aligned} \hat{\sigma} &< \frac{-1}{1-\nu} \\ \hat{S}_{M,0} &= \frac{4\left(\hat{\sigma}+\dfrac{1}{(1-\nu)}\right)}{\nu+(1-\nu^2)\hat{\sigma}} \end{aligned}\right\}. \tag{45}$$

(The reason for the zero value for $\hat{S}_{M,0}$ in the buckled state (ii) is a result of the infinite variety of possible equilibrium shapes under zero load. The stiffness will clearly be zero until any 'slack', represented by the $\hat{\theta}$ term in equation (30), is taken up.)

Equations (43), (44) and (45) have been plotted in Fig. 20, where it is seen that in the buckled states the rigidity first increases sharply as $|\hat{\sigma}|$ increases and then approaches an asymptotic value of $4/(1-\nu^2)$. Such high values for the rigidity result from the induced chordwise curvature, given by

$$\left.\begin{aligned} \hat{\kappa}'_{(ii)} &= -\left(\hat{\sigma}-\frac{1}{(1+\nu)}\right)^{1/2} \\ \hat{\kappa}'_{(iii)} &= +\left(-\hat{\sigma}-\frac{1}{(1-\nu)}\right)^{1/2} \end{aligned}\right\} \tag{46}$$

and will normally be outside any practical range.

4.3. *Pure Torque*.—The condition that $\hat{M}$ is zero and $\hat{T}$ non-zero implies that either

in which case

$$\left.\begin{aligned} \hat{\kappa} &= 0, \\ \hat{T} &= \hat{\theta}\{1-(1+\nu)(\hat{\sigma}-\hat{\theta}^2)\}, \end{aligned}\right\} \tag{47}$$

or

in which case

$$\left.\begin{aligned} 1+(1-\nu)(\hat{\sigma}+\hat{\kappa}^2-\hat{\theta}^2) &= 0, \\ \hat{T} &= \left(\frac{2}{1-\nu}\right)\hat{\theta} \end{aligned}\right\}. \tag{48}$$

A comparison of strain energies shows which of these two states is the correct one. It is then found that if

$$\hat{\sigma} \leqslant \frac{-1}{1-\nu},$$

equation (48) is applicable for all values of $\hat{T}$. But if

$$\hat{\sigma} > \frac{-1}{1-\nu},$$

equation (47) is applicable for values of $|\hat{T}|$ up to a critical value $|\hat{T}^*|$, where

$$\left.\begin{aligned}\hat{T}^* &= \frac{2\hat{\theta}^*}{1-\nu} \\ &= \frac{2}{1-\nu}\left(\hat{\sigma}+\frac{1}{1-\nu}\right)^{1/2}\end{aligned}\right\} \tag{49}$$

and equation (48) is applicable for values of $|\hat{T}|$ greater than $|\hat{T}^*|$. As the torque increases through the critical value of $\hat{T}^*$ the wing buckles and there is a sudden drop in torsional rigidity. This instability is not a type of thermal buckling, although modified by thermal effects; it is simply due to the fact that as the wing twists the middle-surface forces play an increasing part in resisting the torque and there comes a time when the wing will deform into a surface which approximates to a developable surface for then the middle-surface forces will remain constant. The buckled mode of deformation can be determined using the results of equations (23), (48) and (49):

$$\left.\begin{aligned}\hat{\kappa}^2 &= \hat{\theta}^2-(\hat{\theta}^*)^2 \\ \hat{\kappa}' &= \hat{\kappa}\end{aligned}\right\}. \tag{50}$$

It is seen from equation (50) that $\hat{\kappa}$ can be either positive or negative, values which correspond to two distinct modes of buckling; from symmetry there is no preference for either of these modes. The curvatures $\hat{\kappa}$ and $\hat{\kappa}'$ increase rapidly immediately after buckling for we have

$$\left.\begin{aligned}\hat{\kappa} &= \pm\{(\hat{\theta}-\hat{\theta}^*)(\hat{\theta}+\hat{\theta}^*)\}^{1/2} \\ &= \pm\left(\frac{1-\nu}{2}\right)\{(\hat{T}-\hat{T}^*)(\hat{T}+\hat{T}^*)\}^{1/2}\end{aligned}\right\}, \tag{51}$$

which varies as $(\hat{T}-\hat{T}^*)^{1/2}$ immediately after buckling.

When $\hat{T}$ is large compared with $\hat{T}^*$

$$\hat{\kappa}, \hat{\kappa}' \to \pm\hat{\theta}$$

and these relations correspond to modes of deformation which are developable surfaces[10] with generators at ± 45 deg to the spanwise axis. It is to be noticed that such a developable surface is the precise mode of deformation for all values of $\hat{T}$ if $\hat{\sigma} = -1/(1-\nu)$. Some typical torque-twist relationships are shown in Fig. 21.

4.3.1. *Torsional rigidity.*—A non-dimensional measure of the torsional rigidity is afforded by the symbol $\hat{S}_T$ where

$$S_T = \left(\frac{\partial\hat{T}}{\partial\hat{\theta}}\right)_{\hat{M}=\text{const}}, \tag{52}$$

and for the special case of pure torque considered in this paragraph it is obtained by differentiating equations (47) or (48). The initial value of the torsional rigidity (i.e., at $\hat{T}=0$) is determined from this relation using the results of Section 4. As in the flexural case the stiffness depends markedly on whether the wing is in state (i), (ii) or (iii). In the unbuckled state (i) for which

$$\left.\begin{aligned}\frac{-1}{1-\nu} < \hat{\sigma} &< \frac{1}{1+\nu} \\ \text{it can be shown that}\qquad \hat{S}_{T,0} &= 1-(1+\nu)\hat{\sigma}\end{aligned}\right\}. \tag{53}$$

In the buckled state (ii) for which

$$\left.\begin{aligned} \hat{\sigma} &> \frac{1}{1+\nu} \\ \hat{S}_{T,0} &= 2\{\hat{\sigma}(1+\nu)-1\} \\ &\text{or} \quad 0 \end{aligned}\right\}, \tag{54}$$

it can be shown that

and in the buckled state (iii) for which

$$\left.\begin{aligned} \hat{\sigma} &< \frac{-1}{1-\nu} \\ \hat{S}_{T,0} &= \frac{2}{1-\nu} \end{aligned}\right\}. \tag{55}$$

it can be shown that

(The reason for the zero value for $\hat{S}_{T,0}$ in the buckled state (ii) is a result of the infinite variety of possible equilibrium shapes under zero load. The stiffness is zero until any 'slack', represented by the $\hat{\kappa}$ term in equation (30), is taken up.)

Equations (53), (54) and (55) have been plotted in Fig. 20.

4.4. *Bending Moment and Torque Increasing in Fixed Ratio.*—Consider the case in which $\hat{M}$ and $\hat{T}$ increase from zero in such a way that

$$\left.\begin{aligned} \frac{M}{T} &= \phi, \\ \frac{\hat{M}}{\hat{T}} &= \frac{2\phi}{1+\nu} \end{aligned}\right\}. \tag{56}$$

i.e. (from equations (20) or (21))

The relationship between $\hat{T}$ and $\hat{\theta}$ is found by eliminating $\hat{\kappa}$ from equations (26) and (27):

$$\hat{\theta}^2 = \frac{\{(1+\nu)\hat{\sigma}-1+\hat{T}/\hat{\theta}\}\{2-(1-\nu)\hat{T}/\hat{\theta}\}^2}{(1+\nu)[4\phi^2\{1-(1-\nu)\hat{T}/\hat{\theta}\}+\{2-(1-\nu)\hat{T}/\hat{\theta}\}^2]} \tag{57}$$

and the variation of $\hat{\kappa}$ and $\hat{\kappa}'$ with $\hat{T}$ (or $\hat{M}$) follows immediately from equations (27) and (23). The relationships between $\hat{T}$ and $\hat{\theta}$, $\hat{M}$ and $\hat{\kappa}$, and $\hat{M}$ and $\hat{\kappa}'$ are shown in Figs. 22 to 27 for various values of ϕ, assuming $\hat{\sigma} = 0$ or $0{\cdot}5$. It will be noticed that for sufficiently large values of the applied moments the ratios $\hat{T}/\hat{\theta}$, $\hat{M}/\hat{\kappa}$ and $\hat{M}/\hat{\kappa}'$ tend to constant values, values moreover which are independent of $\hat{\sigma}$. The asymptotic value of $\hat{T}/\hat{\theta}$, for example, is determined by the vanishing of the factor in square brackets in equation (57), and is given by

$$\frac{\hat{T}}{\hat{\theta}} \rightarrow \left(\frac{2}{1-\nu}\right)\left(\frac{\sqrt{(1+\phi^2)}}{\phi+\sqrt{(1+\phi^2)}}\right).$$

Similarly it can be shown that

$$\frac{\hat{M}}{\hat{\kappa}} \rightarrow \left(\frac{4}{1-\nu^2}\right)\left(\frac{\phi\sqrt{(1+\phi^2)}}{\{\phi+\sqrt{(1+\phi^2)}\}^2}\right),$$

$$\frac{\hat{M}}{\hat{\kappa}'} \rightarrow \frac{4\phi\sqrt{(1+\phi^2)}}{1-\nu^2}.$$

It will be seen from these asymptotic expressions that

$$\hat{\kappa}\hat{\kappa}' - \hat{\theta}^2 \to 0$$

which represents a developable surface. The angle that the generators of this developable surface make with the chordwise axis is given by

$$\left.\begin{aligned} \tfrac{1}{2}\cot^{-1}\left(\frac{\hat{\kappa}-\hat{\kappa}'}{2\hat{\theta}}\right) &= \tfrac{1}{2}\cot^{-1}\phi \\ &= \tfrac{1}{2}\tan^{-1}\left(\frac{T}{M}\right) \end{aligned}\right\}, \tag{58}$$

which is in agreement with inextensional theory.[10] It can similarly be shown that the stiffness, as well as the deflected shape, tends to the value predicted by inextensional theory as $\hat{M}$ and $\hat{T}$ increase, whatever the value of $\hat{\sigma}$.

5. *Examples.*—The purpose of the following three examples is to indicate the order of magnitude of some of the effects considered here. A more detailed discussion of some of the aero-elastic effects resulting from the change in camber (i.e., $\hat{\kappa}'$) under aerodynamic loading and from the loss of stiffness due to aerodynamic heating is given by Broadbent[11, 12].

(i) A 2 per cent thin Duralumin wing of lenticular parabolic section is subjected to a chordwise parabolic temperature distribution. Assuming $\nu = 0{\cdot}3$ and $\alpha = 2{\cdot}3 \times 10^{-5}$, determine the range of the temperature difference ΔT for which the wing is stable under zero load.

If the wing is solid, it follows from equation (20) that

$$\hat{\sigma} = \frac{\Delta T}{174}$$

so that from Section 4.1 the range of ΔT is

$$\frac{-174}{1-\nu} < \Delta T < \frac{174}{1+\nu},$$

i.e.,

$$-249°\mathrm{C} < \Delta T < 134°\mathrm{C}.$$

Similarly it can be shown from equation (21) that for a thin-walled wing the range is

$$-299°\mathrm{C} < \Delta T < 161°\mathrm{C}.$$

(ii) A 2 per cent thin solid steel wing of lenticular parabolic section is required to withstand a temperature difference ΔT of 300 deg C. Assuming

$$\nu = 0{\cdot}25, \quad \alpha = 1{\cdot}2 \times 10^{-5} \quad \text{and} \quad E = 30 \times 10^6 \text{ lb/sq in.},$$

determine the behaviour of such a wing with and without initial pre-stressing.

With no initial pre-stressing, $\hat{\sigma}$ is given directly by equation (20) whence

$$\hat{\sigma} = 0{\cdot}9.$$

This value for $\hat{\sigma}$ is greater than $1/(1+\nu)$ (i.e., $0{\cdot}8$) and it therefore follows from Section 4.1 that the wing is in the buckled state (ii). The distortion of the wing in this state is given by equation (30),

$$\begin{aligned} \hat{\kappa}^2 + \hat{\theta}^2 &= \hat{\sigma} - \frac{1}{1+\nu} \\ &= 0{\cdot}1. \end{aligned}$$

Now from equation (20)

$$\frac{\kappa}{\hat{\kappa}} = \frac{\theta}{\hat{\theta}} = \frac{0 \cdot 18}{a},$$

so that in terms of κ and θ we have

$$\kappa^2 + \theta^2 = \left(\frac{0 \cdot 057}{a}\right)^2.$$

Thus, if the curvature κ is zero there will be a twist of 3·3 deg over a length equal to the chord; if the twist per unit length θ is zero the curvature over a length equal to the chord will produce a relative deflection of $1 \cdot 4t_0$.

By pre-stressing the wing the values of $\hat{\sigma}$ may be reduced by a fixed amount, so that instead of $\hat{\sigma}$ increasing from zero to 0·9 it may start at $-0 \cdot 6$, say, and increase to 0·3 (a suitable range can be estimated quickly from Fig. 20). The amount and distribution of pre-stressing necessary for this is given by equations (11) and (20). In units of lb/sq in. these equations give

$$10\hat{\sigma}E\left(\frac{t_0}{a}\right)^2\left\{\frac{1}{5} - \left(\frac{2x}{a}\right)^2\right\} = -72{,}000\left\{\frac{1}{5} - \left(\frac{2x}{a}\right)^2\right\},$$

so that the pre-stressing varies parabolically from a compressive stress of 14,400 lb/sq in. at the mid-chord to a tensile stress of 56,600 lb/sq in. at the leading and trailing edges. Such pre-stressing increases the initial value of the torsional rigidity considerably; from equation (53), with $\hat{\sigma} = -0 \cdot 6$,

$$\hat{S}_{T,0} = 1 \cdot 75$$

and as $\hat{\sigma}$ increases to 0·3 the rigidity falls off linearly to the value 0·625. The corresponding values for the flexural rigidity are found from equation (43) to be 1·01 and 0·75.

(iii) At what value of the twist per unit length will torsional instability of an unheated 1 per cent thin solid steel wing occur? From equation (49)

$$\hat{\theta}^* = 1 \cdot 154,$$

which corresponds to a twist of 5·9 deg over a length equal to the chord.

6. *Conclusions.*—A large deflection analysis has been presented for solid and thin-walled wings of biconvex section with a parabolic chordwise temperature distribution. A feature of this class of wing is that under any combination of moment and torque the chordwise curvature is independent of position. This results in a considerable simplification in the analysis and also enables the post-buckling behaviour of the wing to be fully investigated.

Formulae and graphs are presented which enable the distortion of a wing under given moments, torques and thermal stresses to be determined.

Acknowledgment.—The author is indebted to Miss Carol Hollingdale for the extensive computations and for the preparation of the graphs.

LIST OF SYMBOLS (*See* Fig. 1)

Ox, Oy	Cartesian axes, Oy measured spanwise, Ox measured chordwise from the mid-chord of the wing
E, G	Young's modulus, shear modulus (assumed constant)
ν	Poisson's ratio (assumed constant)
α	Coefficient of thermal expansion (assumed constant)
a	Wing chord
t	Wing thickness
$\bar{t}$	Total thickness of spanwise stress-bearing material
h	Skin thickness in thin-walled wing
D	Flexural rigidity per unit width (assumed the same for spanwise and chordwise bending)
T	Chordwise temperature distribution
$T_0, T_1, \Delta T$	Defined by equation (10), in particular
ΔT	Difference between 'the average temperature of the leading and trailing edges' and the mid-chord temperature
ϵ	Spanwise middle-surface strain, measured from a stress-free datum
$\bar{\epsilon}$	Value of ϵ when the wing is flat
$\bar{\epsilon}'$	Defined by equation (4)
$w(x, y)$	Distorted middle surface of wing
$w(x), w$	Chordwise variation of wing distortion defined by equation (1)
M	Applied moment
T	Applied torque
κ	Spanwise curvature
θ	Twist per unit length
κ'	Chordwise curvature (constant for the class of wings considered)
V_m	Strain energy per unit length due to middle-surface strains
V_f	Strain energy per unit length due to flexure and torsion
V	Total strain energy per unit length
A_1, A_2	Constants
$\hat{V}, \hat{\sigma}, \hat{\kappa}, \hat{\theta}, \hat{M}, \hat{T}, \hat{\kappa}'$	Non-dimensional symbols defined by equation (20) or (21)
$\hat{S}_M, \hat{S}_T$	Non-dimensional stiffnesses defined by equations (42) and (52)
μ	Defined by equation (41)
ϕ	M/T

Index * refers to critical buckling conditions.

LIST OF REFERENCES

No.	*Author*	*Title, etc.*
1	H. L. Dryden and J. E. Duberg	Aero-elastic effects of aerodynamic heating. Paper presented to 5th General Assembly, A.G.A.R.D., Ottawa, Canada. June, 1955.
2	L. F. Vosteen and K. E. Fuller	Behaviour of a cantilever plate under rapid-heating conditions. N.A.C.A. Research Memo. L.55E20c. July, 1955.
3	R. L. Bisplinghoff	Some structural and aero-elastic considerations of high-speed flight. *J. Ae. Sci.* April, 1956.
4	N. J. Hoff	Approximate analysis of the reduction in torsional rigidity and torsional buckling of solid wings under thermal stresses. *J. Ae. Sci.* June, 1956.
5	B. Budiansky and J. Mayers ..	Influence of aerodynamic heating on the effective torsional stiffness of thin wings. *J. Ae. Sci.* December, 1956.
6	S. L. Kochanski and J. H. Argyris	Some effects of kinetic heating on the stiffness of thin wings. Parts I and II. *Aircraft Engineering*. October, 1957 and February, 1958.
7	E. H. Mansfield	The influence of aerodynamic heating on the flexural rigidity of a thin wing. R. & M. 3115. September, 1957.
8	S. Timoshenko	*Theory of Plates and Shells.* McGraw-Hill. 1940.
9	H. and B. S. Jeffreys	*Methods of Mathematical Physics.* 2nd Edition. Cambridge. 1950.
10	E. H. Mansfield	The inextensional theory for thin flat plates. *Quart. J. Mech. App. Math.* Vol. VIII. Pt 3. 1955.
11	E. G. Broadbent	Aero-elastic problems associated with high speed and high temperature. *J. R. Ae. Soc.* December, 1958.
12	E. G. Broadbent	Flutter of an untapered wing allowing for thermal effects. C.P. No. 442, April, 1959

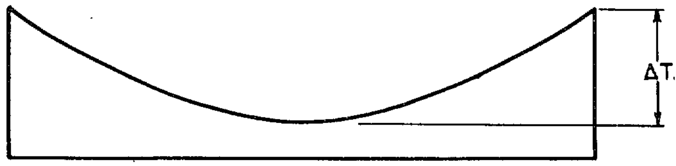

PARABOLIC CHORDWISE TEMPERATURE DISTRIBUTION.

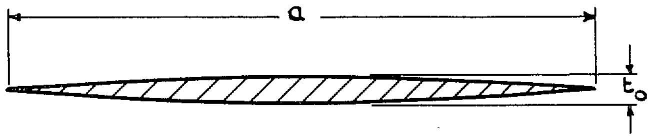

$$\hat{\sigma} = \frac{a^2 \alpha \Delta T}{10 t_o^2}$$

$$\frac{\hat{K}}{K} = \frac{\hat{\theta}}{\theta} = \frac{\hat{K}'}{K'} = \frac{a^2}{(4\sqrt{5})t_o}$$

$$\frac{\hat{M}}{M} = \left(\frac{2}{1+\nu}\right)\frac{\hat{T}}{T} = \frac{(21\sqrt{5})a}{16 E t_o^4}$$

NOTATION FOR SOLID WING.

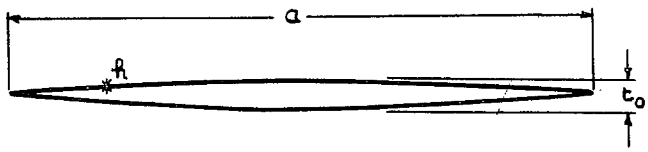

$$\hat{\sigma} = \frac{a^2 \alpha \Delta T}{12 t_o^2}$$

$$\frac{\hat{K}}{K} = \frac{\hat{\theta}}{\theta} = \frac{\hat{K}'}{K'} = \frac{a^2}{(4\sqrt{6})t_o}$$

$$\frac{\hat{M}}{M} = \left(\frac{2}{1+\nu}\right)\frac{\hat{T}}{T} = \frac{(5\sqrt{6})a}{32 E h t_o^3}$$

NOTATION FOR THIN-WALLED WING.

FIG. 1. Figure showing wing sections considered and notation.

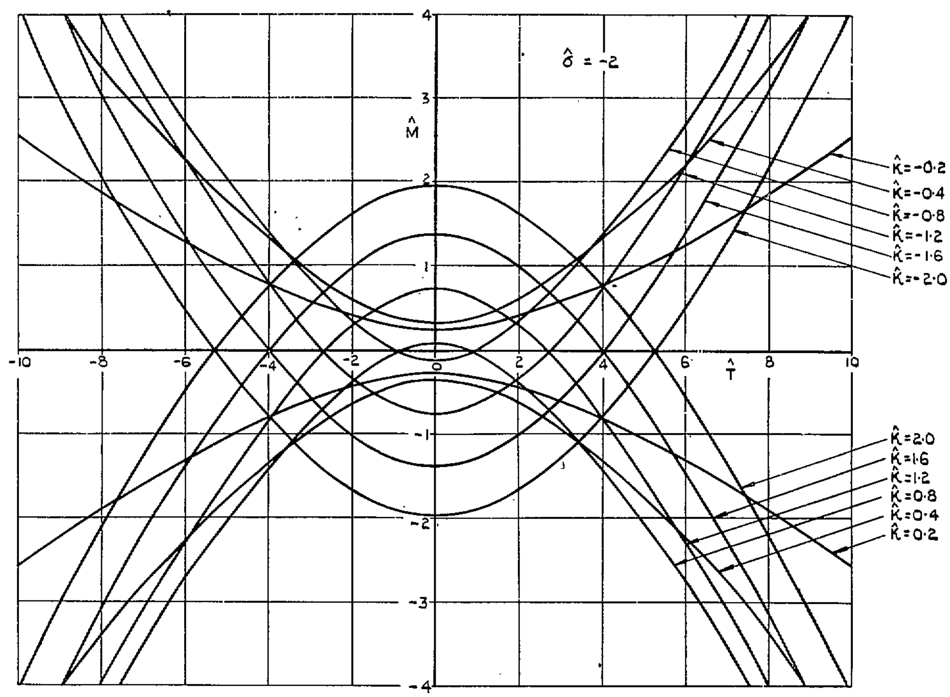

FIG. 2. Variation of curvature $\hat{\kappa}$ with torque $\hat{T}$ and moment $\hat{M}$ (Temperature-stress parameter $\hat{\sigma} = -2$).

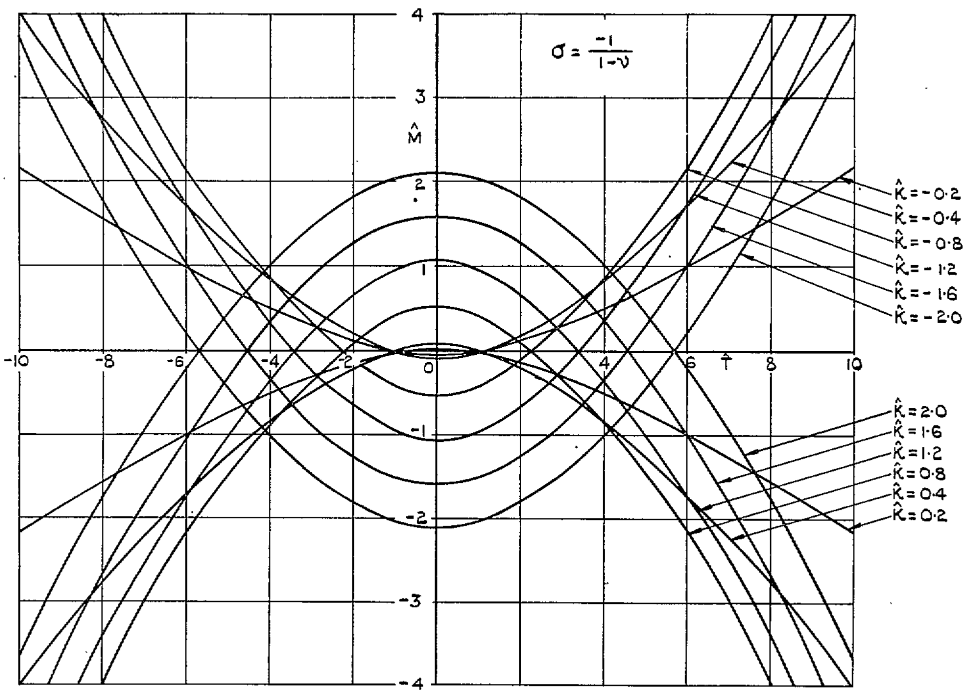

FIG. 3. Variation of curvature $\hat{\kappa}$ with torque $\hat{T}$ and moment $\hat{M}$ (Temperature-stress parameter $\hat{\sigma} = -1{\cdot}43$).

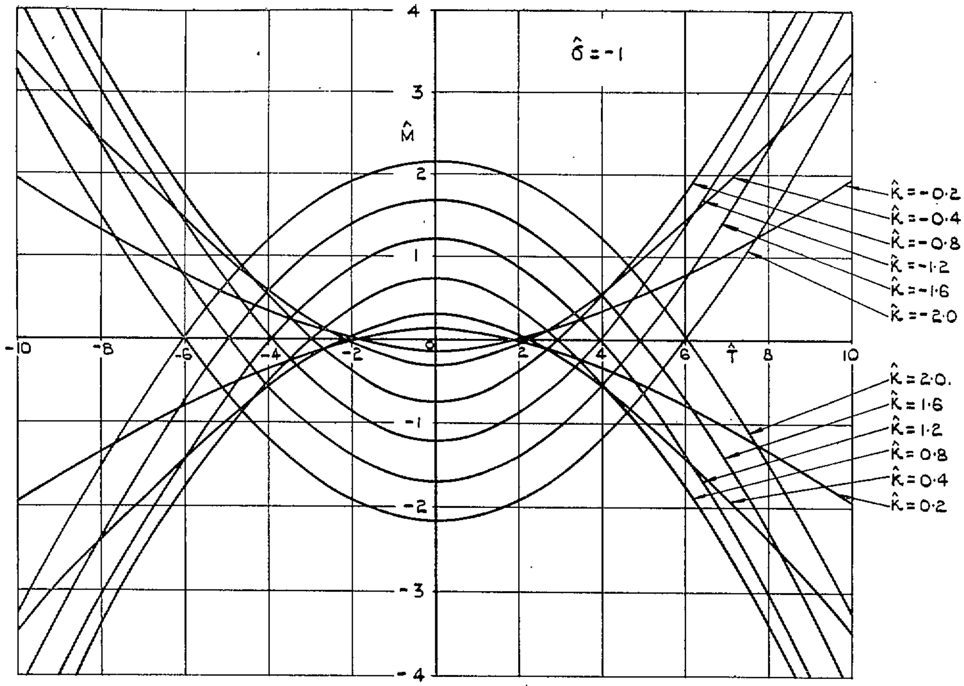

FIG. 4. Variation of curvature $\hat{\kappa}$ with torque $\hat{T}$ and moment $\hat{M}$ (Temperature-stress parameter $\hat{\sigma} = -1$).

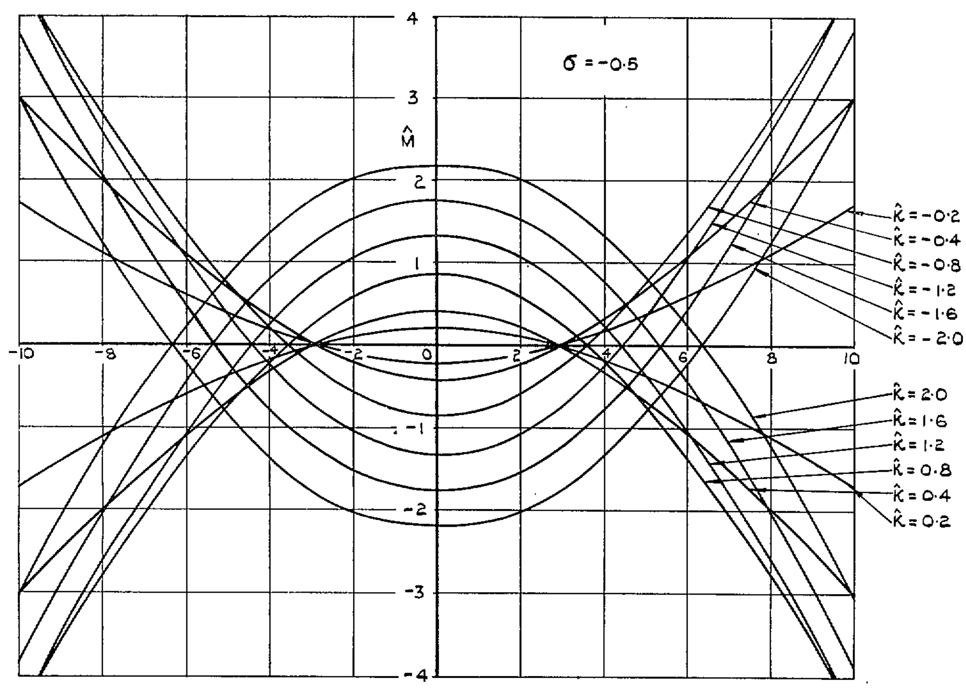

FIG. 5. Variation of curvature $\hat{\kappa}$ with torque $\hat{T}$ and moment $\hat{M}$ (Temperature-stress parameter $\hat{\sigma} = -0{\cdot}5$).

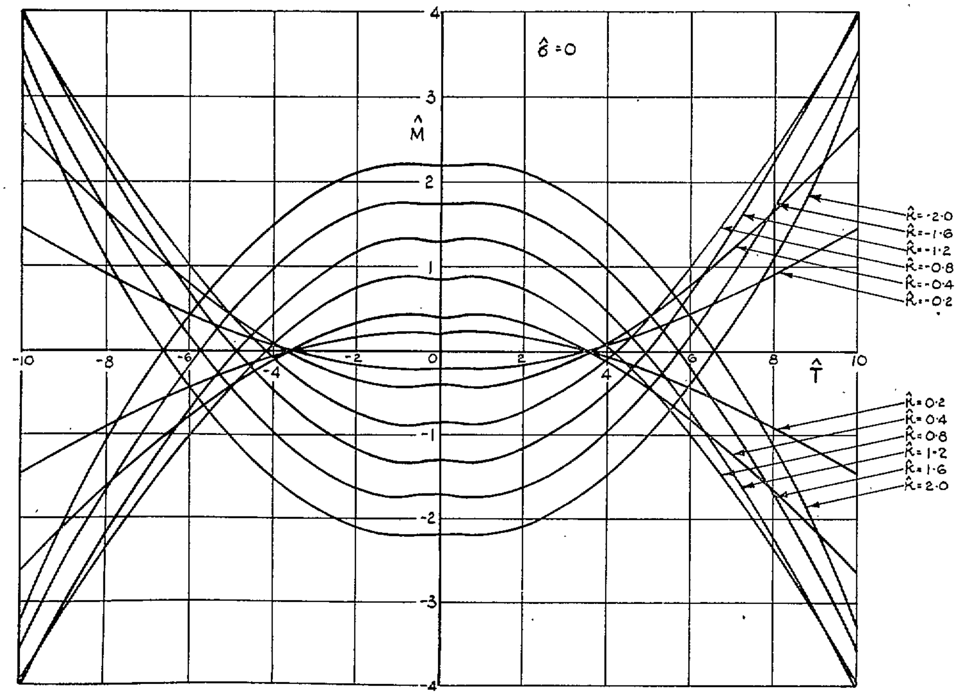

FIG. 6. Variation of curvature $\hat{\kappa}$ with torque $\hat{T}$ and moment $\hat{M}$ (Temperature-stress parameter $\hat{\sigma} = 0$).

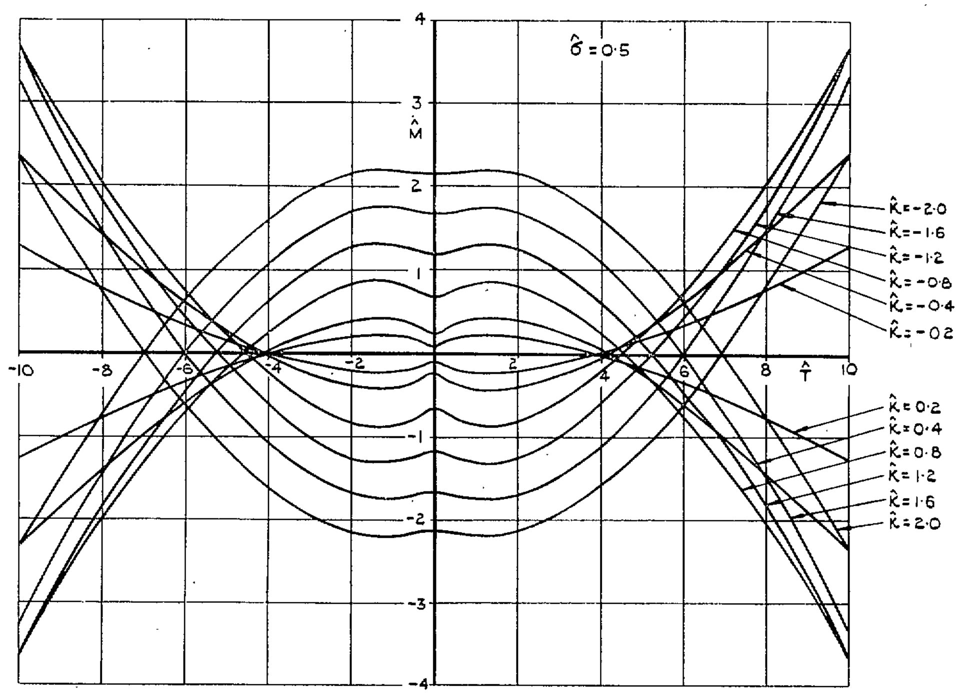

FIG. 7. Variation of curvature $\hat{\kappa}$ with torque $\hat{T}$ and moment $\hat{M}$ (Temperature-stress parameter $\hat{\sigma} = 0{\cdot}5$).

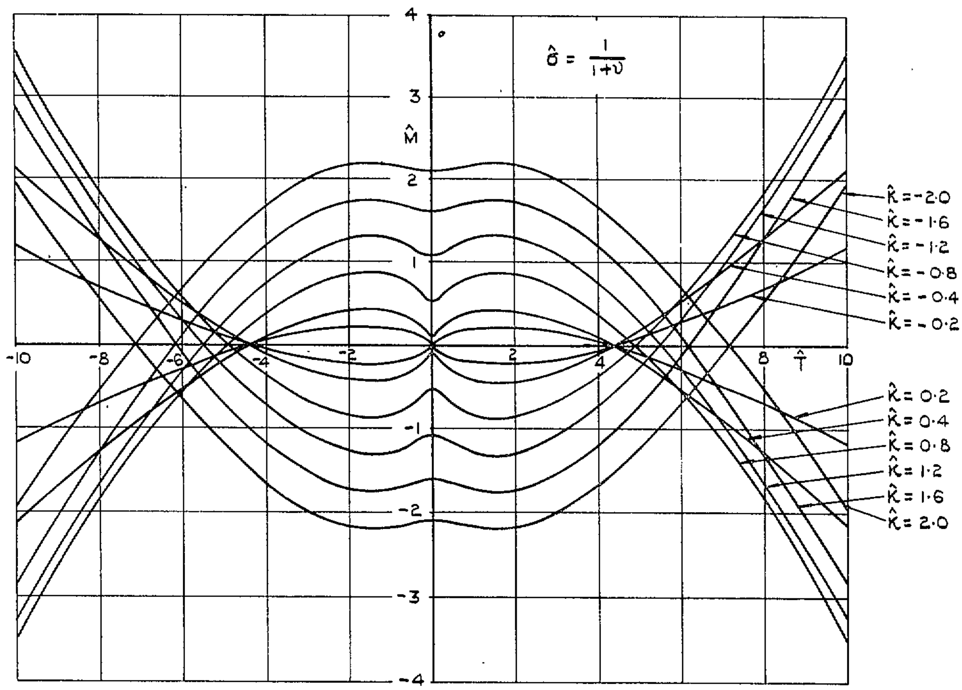

FIG. 8. Variation of curvature $\hat{\kappa}$ with torque $\hat{T}$ and moment $\hat{M}$ (Temperature-stress parameter $\hat{\sigma} = 0{\cdot}77$).

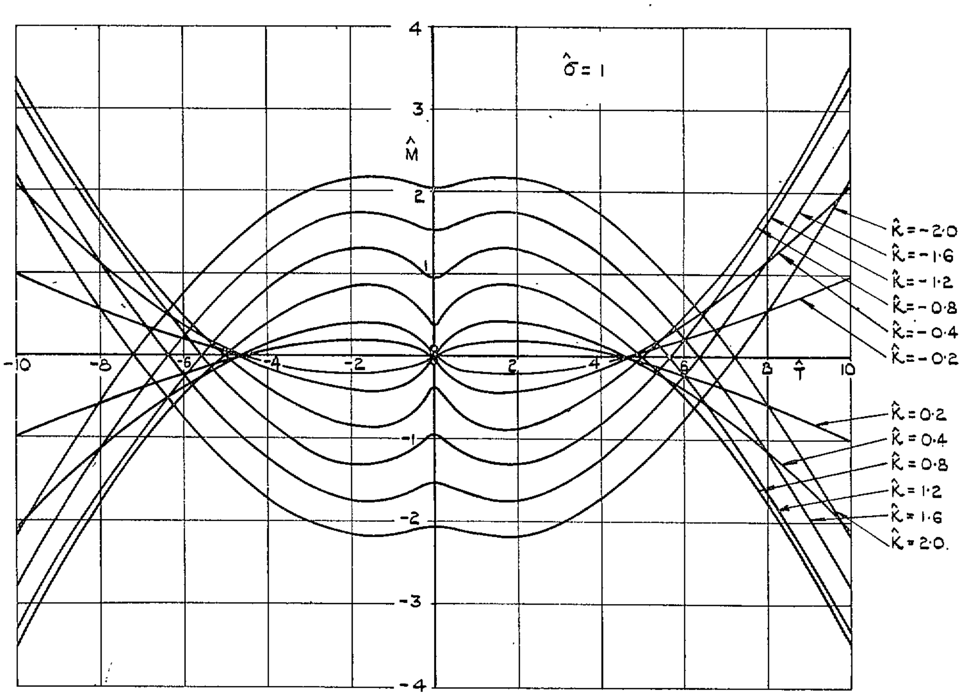

FIG. 9. Variation of curvature $\hat{\kappa}$ with torque $\hat{T}$ and moment $\hat{M}$ (Temperature-stress parameter $\hat{\sigma} = 1$).

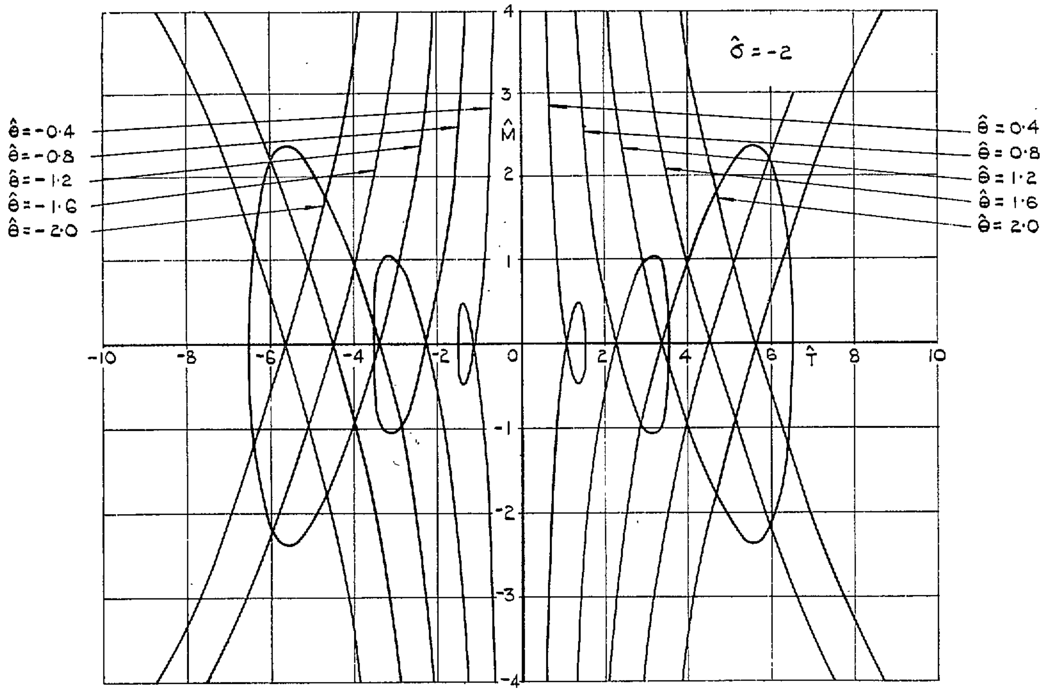

FIG. 10. Variation of twist per unit length $\hat{\theta}$ with torque $\hat{T}$ and moment $\hat{M}$ (Temperature-stress parameter $\hat{\sigma} = -2$).

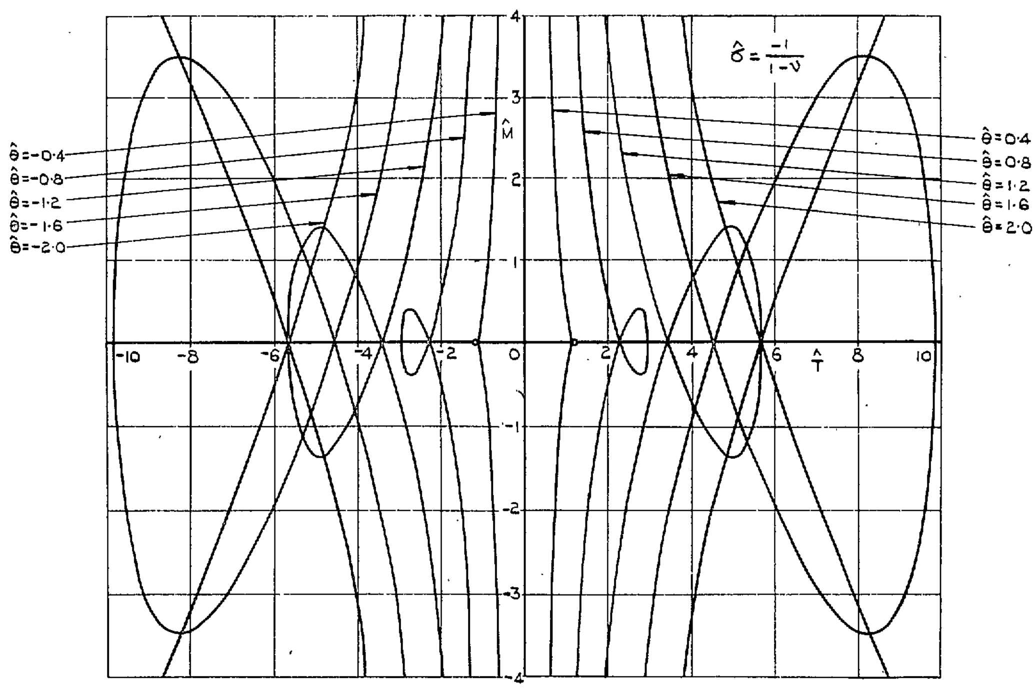

FIG. 11. Variation of twist per unit length $\hat{\theta}$ with torque $\hat{T}$ and moment $\hat{M}$ (Temperature-stress parameter $\hat{\sigma} = -1{\cdot}43$).

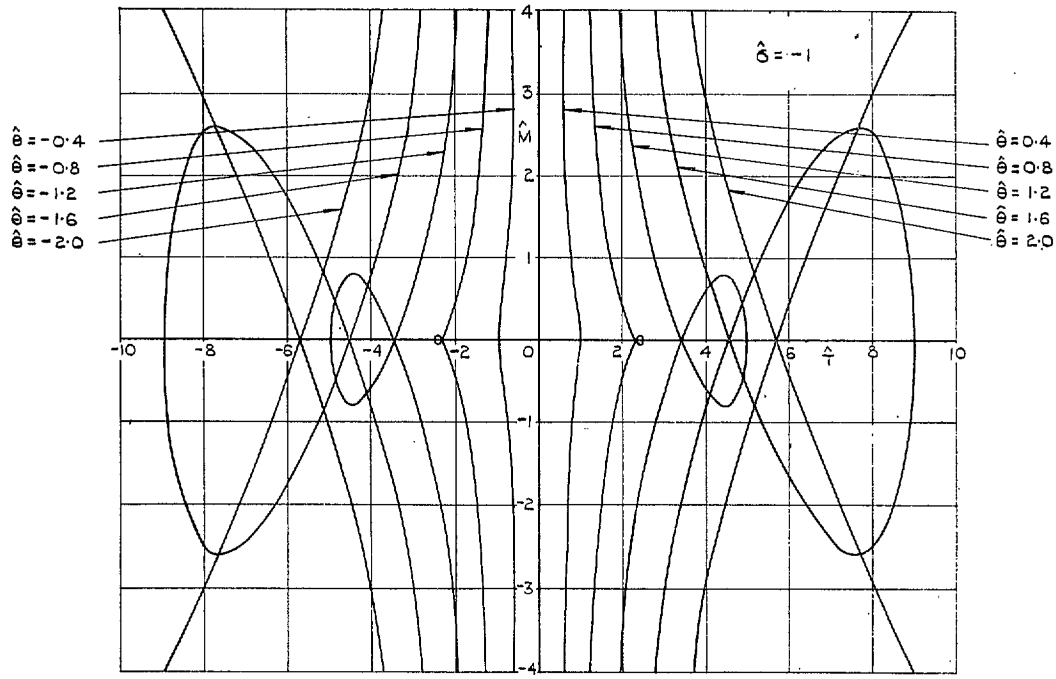

FIG. 12. Variation of twist per unit length $\hat{\theta}$ with torque $\hat{T}$ and moment $\hat{M}$ (Temperature-stress parameter $\hat{\sigma} = -1$).

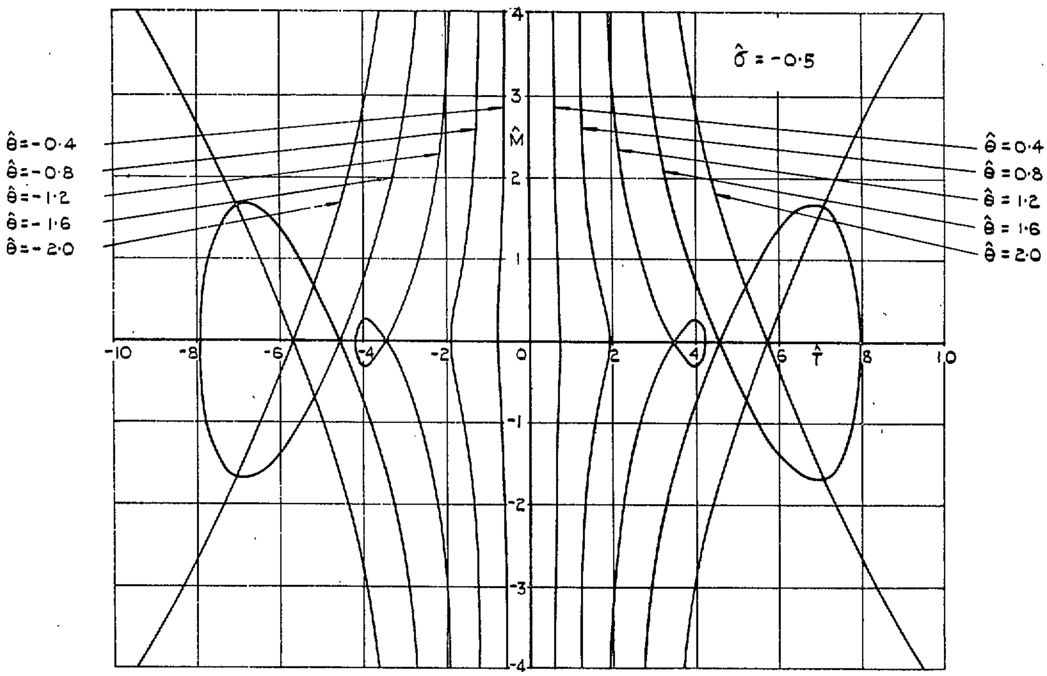

FIG. 13. Variation of twist per unit length $\hat{\theta}$ with torque $\hat{T}$ and moment $\hat{M}$ (Temperature-stress parameter $\hat{\sigma} = -0{\cdot}5$).

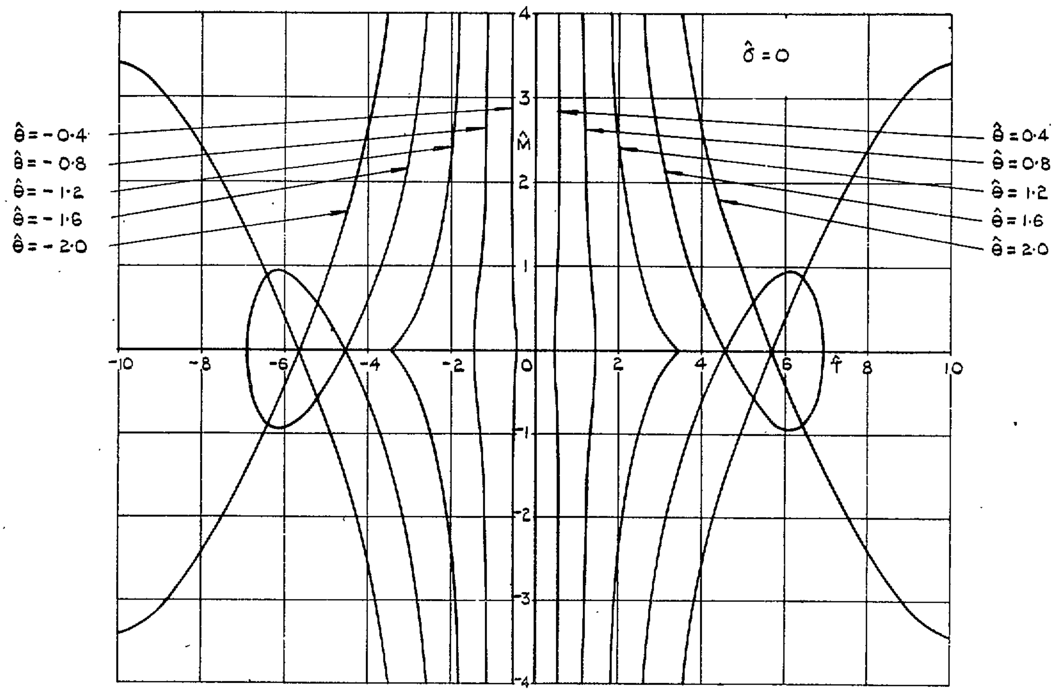

FIG. 14. Variation of twist per unit length $\hat{\theta}$ with torque $\hat{T}$ and moment $\hat{M}$ (Temperature-stress parameter $\hat{\sigma} = 0$).

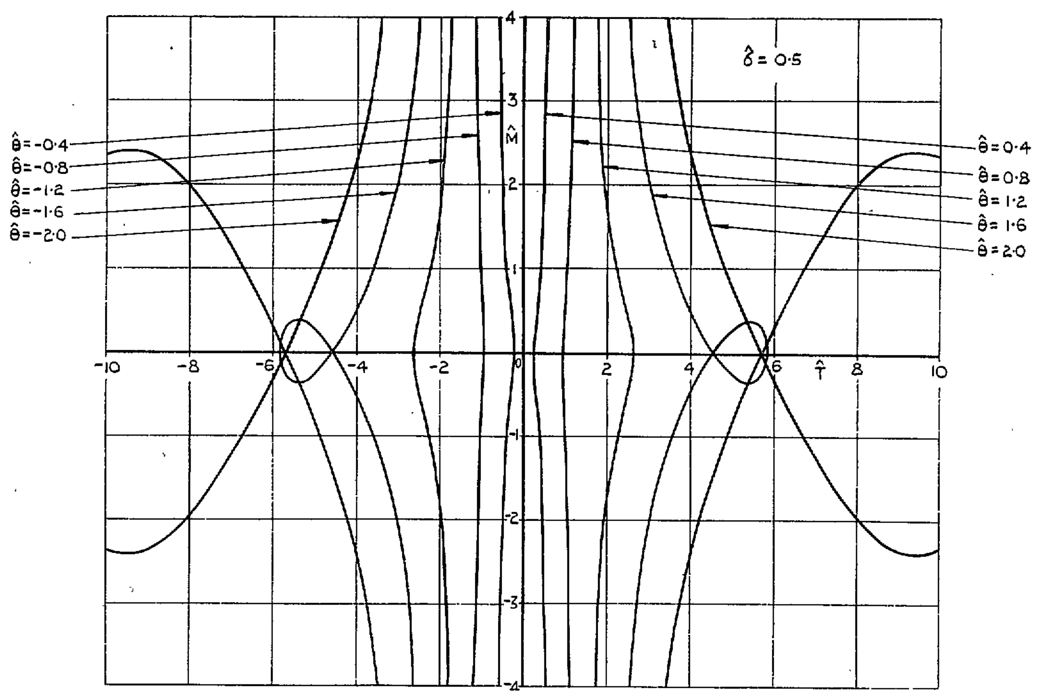

FIG. 15. Variation of twist per unit length $\hat{\theta}$ with torque $\hat{T}$ and moment $\hat{M}$ (Temperature-stress parameter $\hat{\sigma} = 0{\cdot}5$).

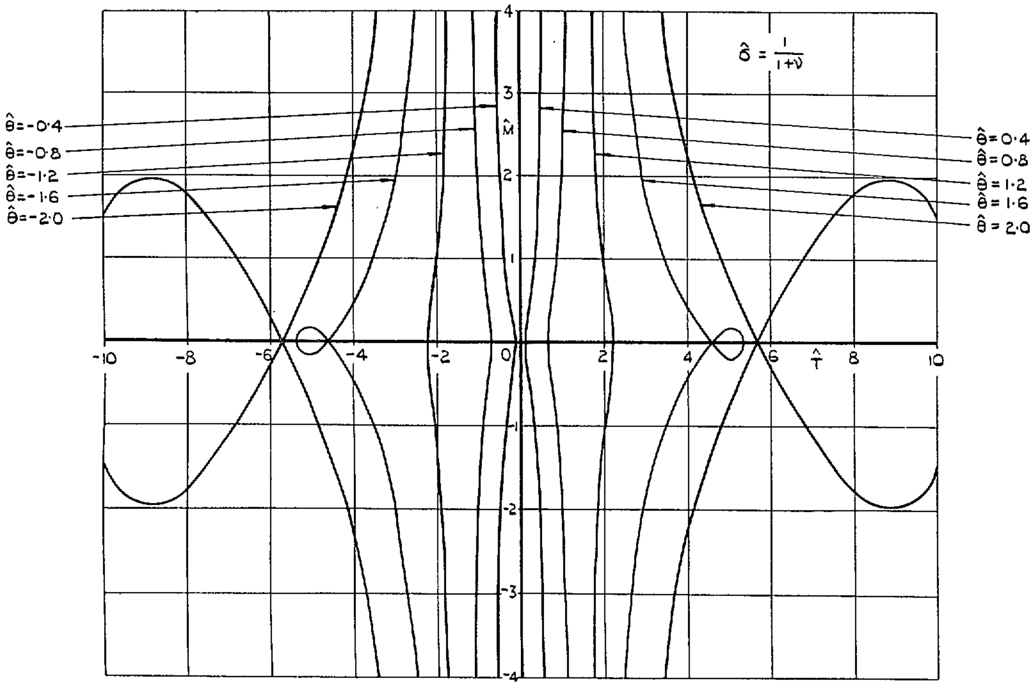

FIG. 16. Variation of twist per unit length $\hat{\theta}$ with torque $\hat{T}$ and moment $\hat{M}$ (Temperature-stress parameter $\hat{\sigma} = 0{\cdot}77$).

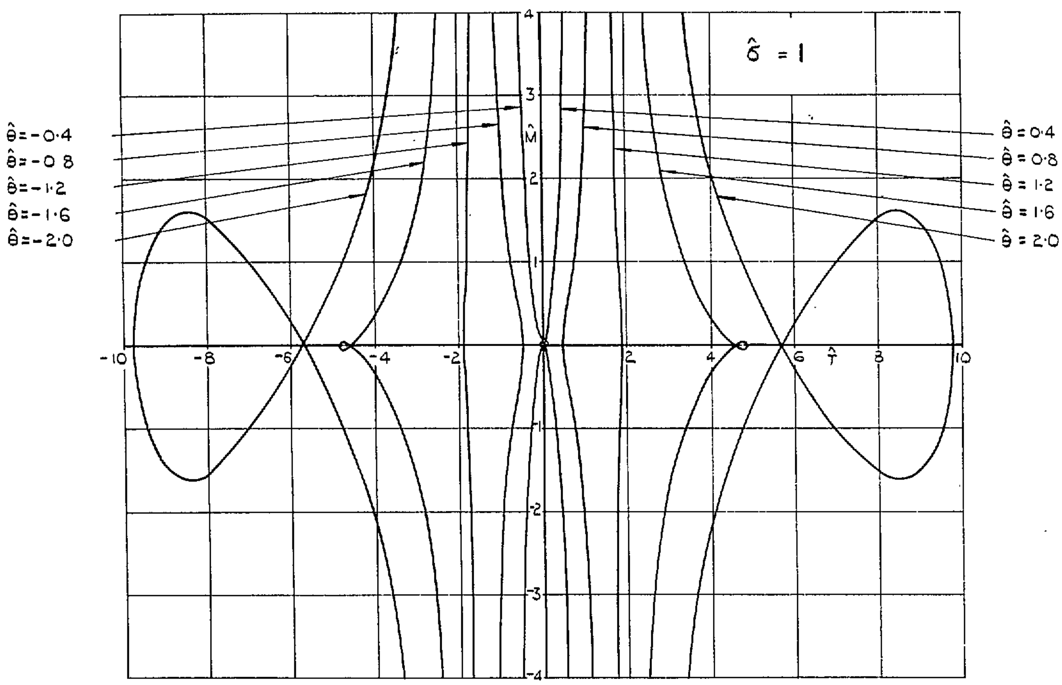

FIG. 17. Variation of twist per unit length $\hat{\theta}$ with torque $\hat{T}$ and moment $\hat{M}$ (Temperature-stress parameter $\hat{\sigma} = 1$).

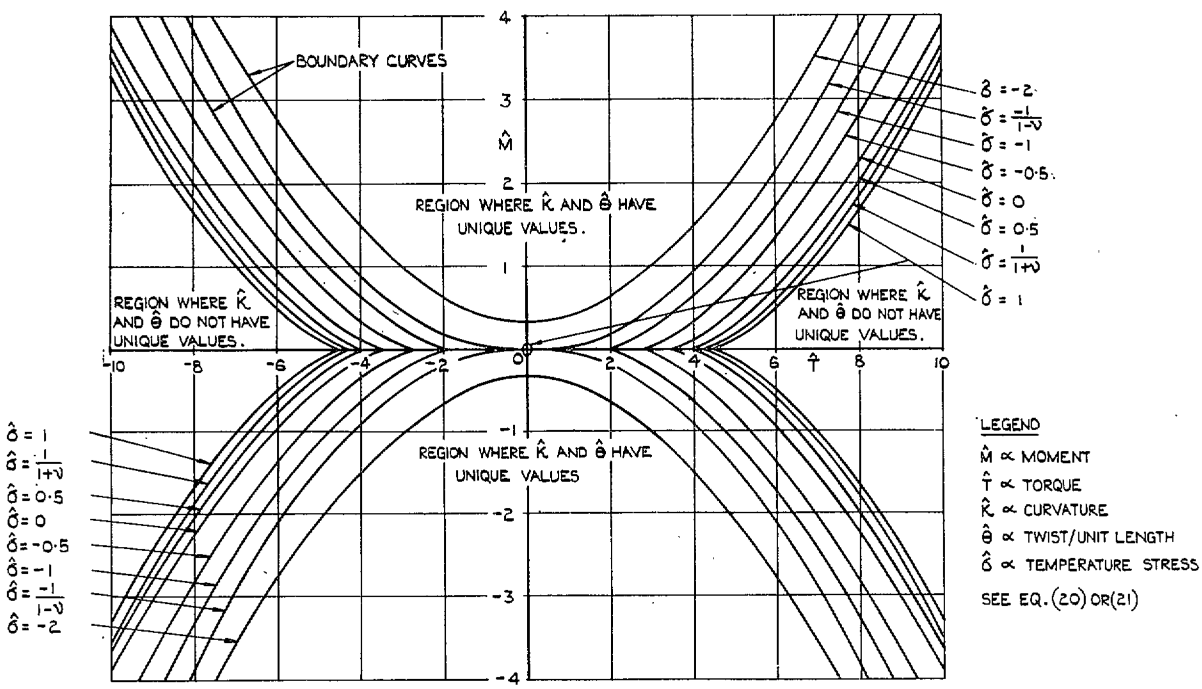

FIG. 18. Regions in the $\hat{M}$, $\hat{T}$ plane in which $\hat{\kappa}$ and $\hat{\theta}$ do not have unique values.

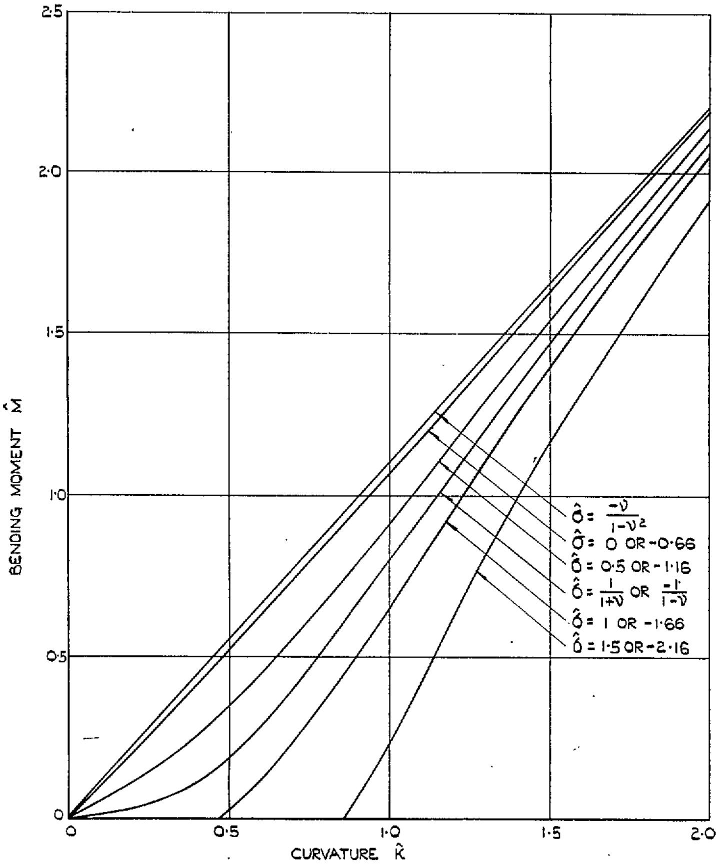

FIG. 19. Bending moment-curvature relationships for various values of temperature-stress parameter $\hat{\sigma}$.

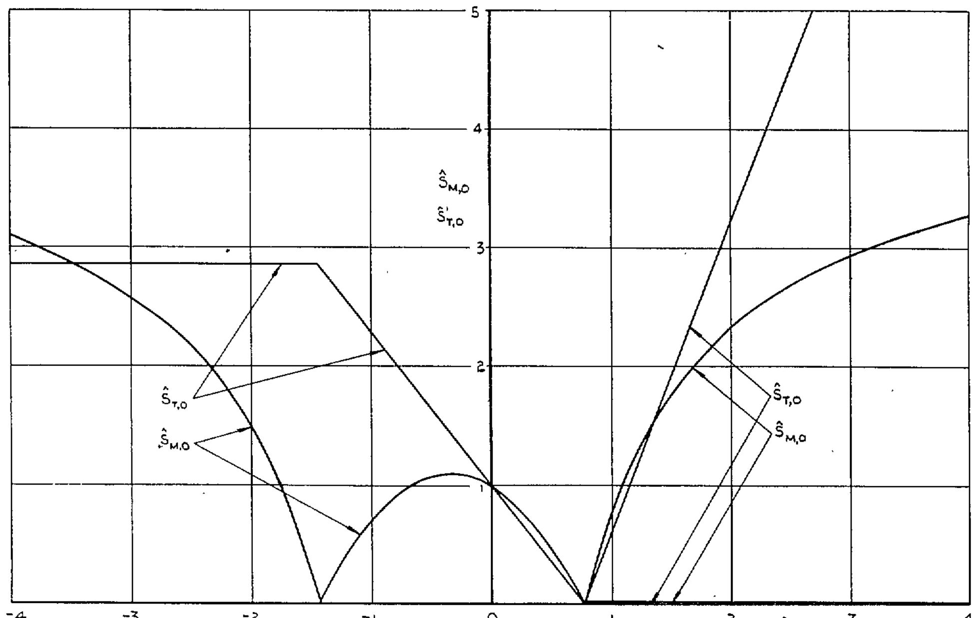

FIG. 20. Initial values of the flexural and torsional rigidities $\hat{S}_{M,0}$ and $\hat{S}_{T,0}$ (Variation with temperature-stress parameter $\hat{\sigma}$).

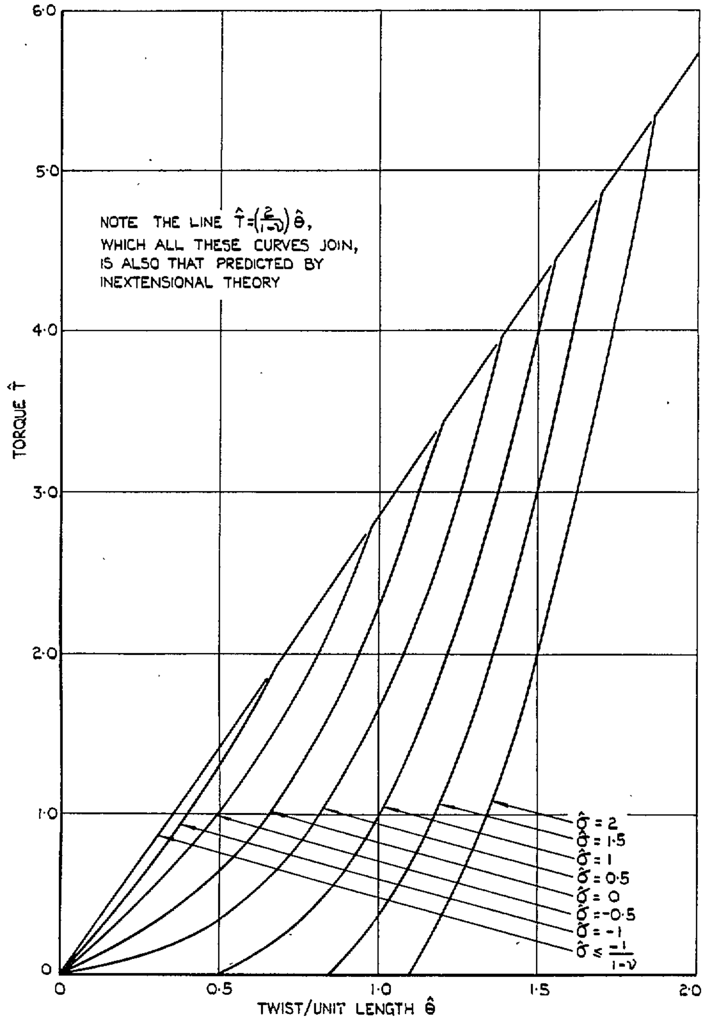

FIG. 21. Torque-twist relationships for various values of temperature-stress parameter $\hat{\sigma}$.

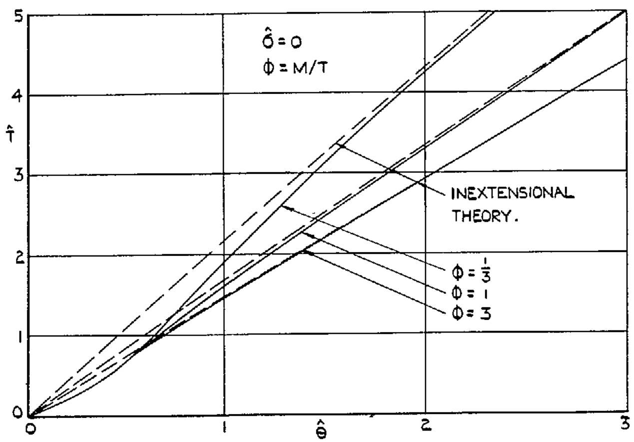

FIG. 22. Variation of twist per unit length $\hat{\theta}$ with torque $\hat{T}$ (Temperature-stress parameter $\hat{\sigma} = 0$).

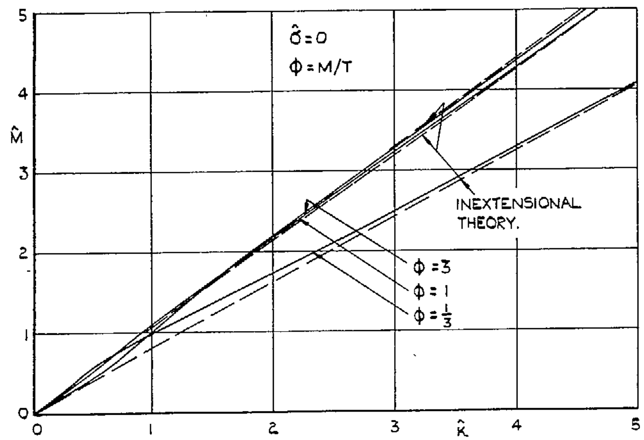

FIG. 24. Variation of longitudinal curvature $\hat{\kappa}$ with moment $\hat{M}$ (Temperature-stress parameter $\hat{\sigma} = 0$).

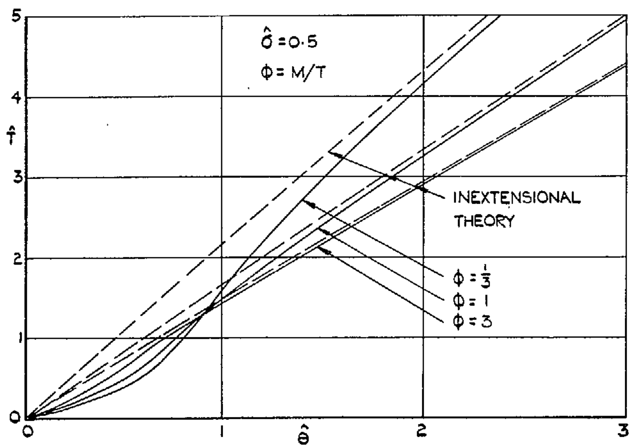

FIG. 23. Variation of twist per unit length $\hat{\theta}$ with torque $\hat{T}$ (Temperature-stress parameter $\hat{\sigma} = 0{\cdot}5$).

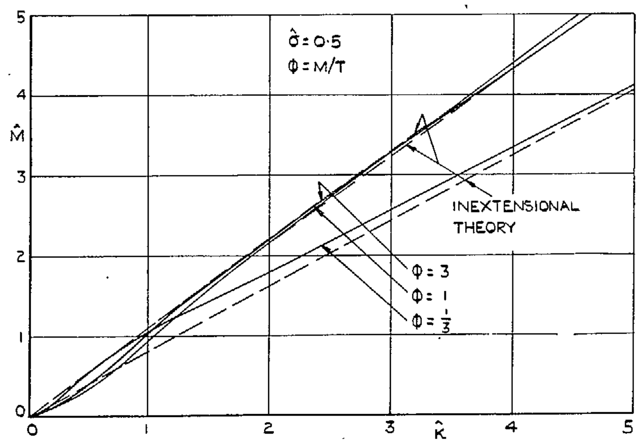

FIG. 25. Variation of longitudinal curvature $\hat{\kappa}$ with moment $\hat{M}$ (Temperature-stress parameter $\hat{\sigma} = 0{\cdot}5$).

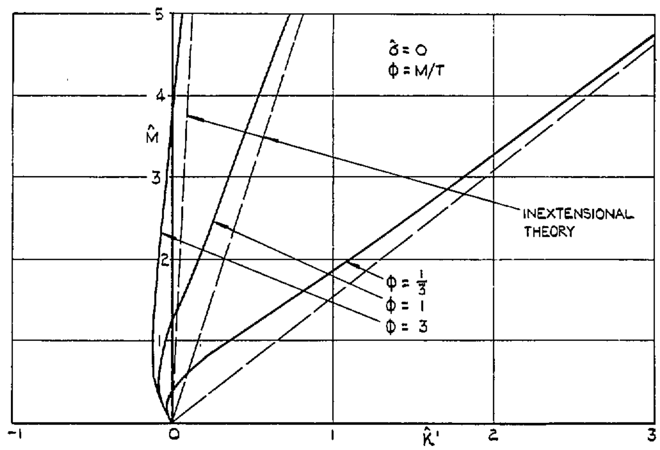

FIG. 26. Variation of chordwise curvature $\hat{\kappa}'$ with moment $\hat{M}$ (Temperature-stress parameter $\hat{\sigma} = 0$).

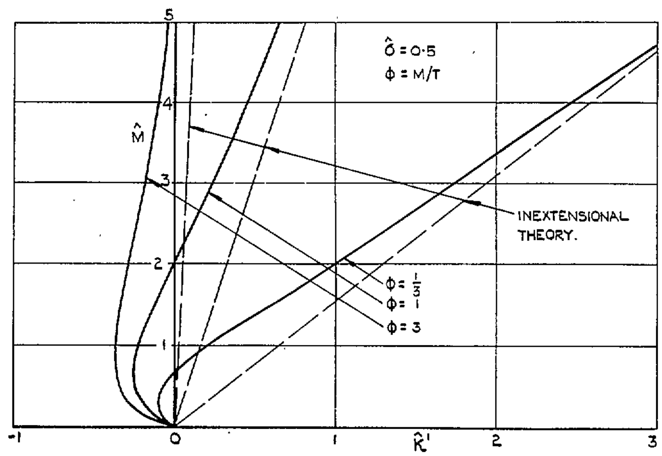

FIG. 27. Variation of chordwise curvature $\hat{\kappa}'$ with moment $\hat{M}$ (Temperature-stress parameter $\hat{\sigma} = 0{\cdot}5$).

Wt. 66 K.5.

Printed in England under the authority of Her Majesty's Stationery Office by John Wright & Sons Ltd. at the Stonebridge Press, Bristol

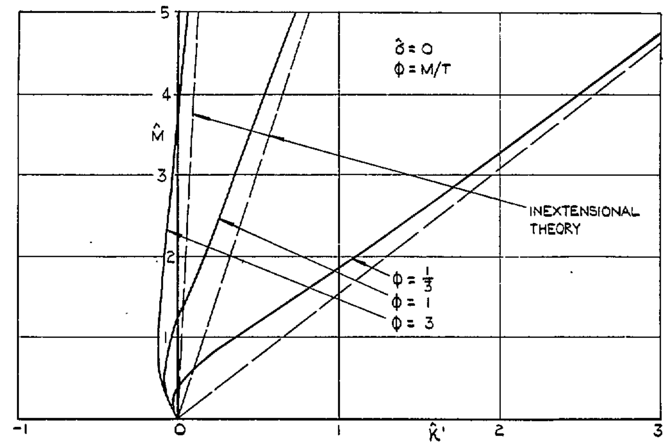

FIG. 26. Variation of chordwise curvature $\hat{\kappa}'$ with moment $\hat{M}$ (Temperature-stress parameter $\hat{\sigma} = 0$).

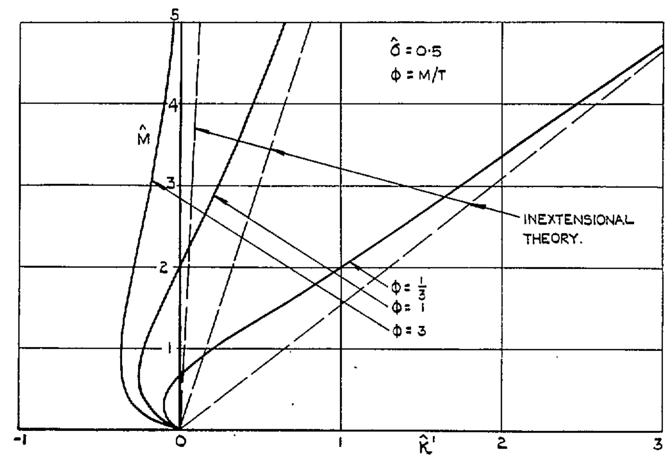

FIG. 27. Variation of chordwise curvature $\hat{\kappa}'$ with moment $\hat{M}$ (Temperature-stress parameter $\hat{\sigma} = 0{\cdot}5$).

Wt. 66 K.5.

Printed in England under the authority of Her Majesty's Stationery Office by John Wright & Sons Ltd. at the Stonebridge Press, Bristol

Publications of the Aeronautical Research Council

ANNUAL TECHNICAL REPORTS OF THE AERONAUTICAL RESEARCH COUNCIL (BOUND VOLUMES)

1941 Aero and Hydrodynamics, Aerofoils, Airscrews, Engines, Flutter, Stability and Control, Structures. 63s. (post 2s. 3d.)

1942 Vol. I. Aero and Hydrodynamics, Aerofoils, Airscrews, Engines. 75s. (post 2s. 3d.)
Vol. II. Noise, Parachutes, Stability and Control, Structures, Vibration, Wind Tunnels. 47s. 6d. (post 1s. 9d.)

1943 Vol. I. Aerodynamics, Aerofoils, Airscrews. 80s. (post 2s.)
Vol. II. Engines, Flutter, Materials, Parachutes, Performance, Stability and Control, Structures. 90s. (post 2s. 3d.)

1944 Vol. I. Aero and Hydrodynamics, Aerofoils, Aircraft, Airscrews, Controls. 84s. (post 2s. 6d.)
Vol. II. Flutter and Vibration, Materials, Miscellaneous, Navigation, Parachutes, Performance, Plates and Panels, Stability, Structures, Test Equipment, Wind Tunnels. 84s. (post 2s. 6d.)

1945 Vol. I. Aero and Hydrodynamics, Aerofoils. 130s. (post 3s.)
Vol. II. Aircraft, Airscrews, Controls. 130s. (post 3s.)
Vol. III. Flutter and Vibration, Instruments, Miscellaneous, Parachutes, Plates and Panels, Propulsion. 130s. (post 2s. 9d.)
Vol. IV. Stability, Structures, Wind Tunnels, Wind Tunnel Technique. 130s. (post 2s. 9d.)

1946 Vol. I. Accidents, Aerodynamics, Aerofoils and Hydrofoils. 168s. (post 3s. 3d.)
Vol. II. Airscrews, Cabin Cooling, Chemical Hazards, Controls, Flames, Flutter, Helicopters, Instruments and Instrumentation, Interference, Jets, Miscellaneous, Parachutes. 168s. (post 2s. 9d.)
Vol. III. Performance, Propulsion, Seaplanes, Stability, Structures, Wind Tunnels. 168s. (post 3s. 6d.)

1947 Vol. I. Aerodynamics, Aerofoils, Aircraft. 168s. (post 3s. 3d.)
Vol. II. Airscrews and Rotors, Controls, Flutter, Materials, Miscellaneous, Parachutes, Propulsion, Seaplanes, Stability, Structures, Take-off and Landing. 168s. (post 3s. 3d.)

Special Volumes

Vol. I. Aero and Hydrodynamics, Aerofoils, Controls, Flutter, Kites, Parachutes, Performance, Propulsion, Stability. 126s. (post 2s. 6d.)
Vol. II. Aero and Hydrodynamics, Aerofoils, Airscrews, Controls, Flutter, Materials, Miscellaneous, Parachutes, Propulsion, Stability, Structures. 147s. (post 2s. 6d.)
Vol. III. Aero and Hydrodynamics, Aerofoils, Airscrews, Controls, Flutter, Kites, Miscellaneous, Parachutes, Propulsion, Seaplanes, Stability, Structures, Test Equipment. 189s. (post 3s. 3d.)

Reviews of the Aeronautical Research Council

1939–48 3s. (post 5d.) 1949–54 5s. (post 5d.)

Index to all Reports and Memoranda published in the Annual Technical Reports

1909–47 R. & M. 2600 6s. (post 2d.)

Indexes to the Reports and Memoranda of the Aeronautical Research Council

Between Nos. 2351–2449	R. & M. No. 2450	2s. (post 2d.)
Between Nos. 2451–2549	R. & M. No. 2550	2s. 6d. (post 2d.)
Between Nos. 2551–2649	R. & M. No. 2650	2s. 6d. (post 2d.)
Between Nos. 2651–2749	R. & M. No. 2750	2s. 6d. (post 2d.)
Between Nos. 2751–2849	R. & M. No. 2850	2s. 6d. (post 2d.)
Between Nos. 2851–2949	R. & M. No. 2950	3s. (post 2d.)

HER MAJESTY'S STATIONERY OFFICE

from the addresses overleaf

Published by
HER MAJESTY'S STATIONERY OFFICE

To be purchased from
York House, Kingsway, London W.C.2
423 Oxford Street, London W.1
13A Castle Street, Edinburgh 2
109 St. Mary Street, Cardiff
39 King Street, Manchester 2
50 Fairfax Street, Bristol 1
2 Edmund Street, Birmingham 3
80 Chichester Street, Belfast 1
or through any bookseller

R. & M. No. 3195

S.O. Code No. 23-3195